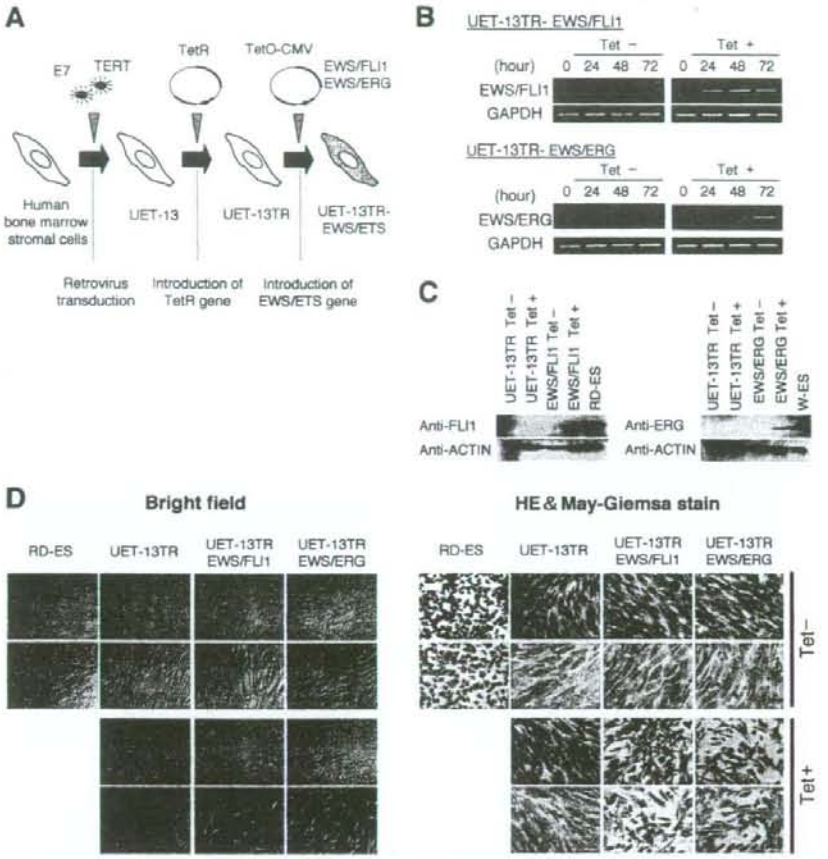

FIG. 1. The effect of EWS/ETS on the morphology of UET-13 cells. (A) The establishment of a tetracycline-inducible EWS/ETS expression system in UET-13 cells. CMV, cytomegalovirus. (B) Analyses for confirming the inducible expression of EWS/ETS genes. EWS/ETS mRNAs were detected in UET-13 transfectants UET-13TR-EWS/FLI1 and UET-13TR-EWS/ERG by RT-PCR. These cells were treated with or without 3 μg/ml of tetracycline (Tet) for the indicated periods. As an internal control, a human GAPDH gene was used. (C) Analyses for confirming the inducible expression of EWS/ETS proteins. The cells were treated as described for panel B and subjected to Western blotting for the detection of EWS/ETS proteins. The extracts of RD-ES and W-ES cells were also examined as positive controls. Membranes were reprobed with anti-actin antibody as a loading control. (D) Morphological change after tetracycline treatment of UET-13 transfectants. UET-13 cells and the transfectants were cultured in the absence or presence of tetracycline for 72 h and observed by light microscopy. Magnification, ×40 (top); ×200 (bottom). Cells were also examined using hematoxylin-eosin (HE) (top) and May-Giemsa (bottom) staining (magnification, ×200).

Real-time RT-PCR. Real-time RT-PCR was performed using TaqMan universal PCR master mix and TaqMan gene expression assays and an inventoried assay on an ABI Prism 7900HT sequence detection system (Applied Biosystems) according to the manufacturer's instructions. The human GAPDH gene was used as an internal control for normalization.

DNA microarray analysis. Total RNA isolated from cells was reverse transcribed and labeled using one-cycle target labeling and control reagents as instructed by the manufacturer (Affymetrix). The labeled probes were hybridized to the human genome U133 Plus 2.0 array (Affymetrix). The arrays were performed in a single experiment and analyzed using GeneChip operating software, version 1.2 (Affymetrix). Background subtraction, normalization, and principal component analysis (PCA) were performed by GeneSpring GX 7.3 software (Agilent Technologies). Signal intensities were prenormalized based on the median of all measurements on that chip. To account for the difference in detection efficiencies between the spots, prenormalized signal intensities on each gene were normalized to the median of prenormalized measurements for that gene. The data were filtered using the following steps. (i) Genes that were scored as absent in all samples were eliminated. (ii) Genes for which the signal intensities were lower than 100 were eliminated. (iii) Performing cluster analysis using filtering genes, we selected the genes that exhibited increased expression or decreased expression in tetracycline-treated cells. Accession numbers for the microarray data are given below.

Invasion assay. The invasion assay was performed using Matrigel (BD Bioscience) according to the previous description (34) with some modification. Polycarbonate filter inserts containing 8-μm pores (BD Falcon) were coated with 50 μl of a 6:1 mixture of culture medium and Matrigel and placed into 24-well culture plates containing DMEM supplemented with 10% T-FBS as chemoattractants. Cells (2.5×10^4) treated with or without tetracycline for 72 h were suspended in DMEM containing 0.01% T-FBS and plated on top of each filter insert. After 20 h in culture in the presence or absence of tetracycline, noninvading cells were removed from upper surface of the filter with a cotton swab. The invading cells on the lower surface of the filter were fixed with formalin, stained with hematoxylin-eosin, and counted in five fields per membrane with light microscopy. As a control, cells were also cultured on uncoated filter inserts. The invasion efficiency was presented as the ratio of the number of invading cells on Matrigel-coated inserts to that on uncoated inserts. Experiments were performed in triplicate, and the means with standard deviations of the values are shown in the graphs in Fig. 8.

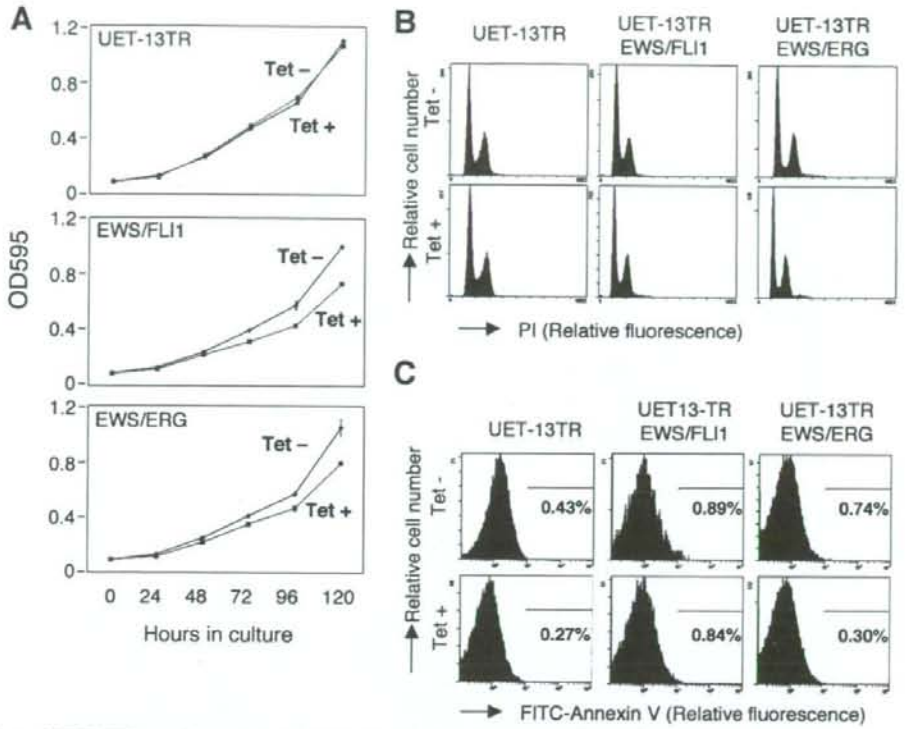

FIG. 2. Effects of EWS/ETS on cell growth in UET-13 cells. (A) Growth curve for UET-13 transfectants. Cells were seeded at 10^3/well and cultured as described for Fig. 1. The increase in cell number was analyzed by MTT assay. Values are means with the standard errors (SE) from three independent experiments. Diamond symbols indicate UET-13 transfectants in the absence of tetracycline (Tet); box symbols indicate UET-13 transfectants in the presence of tetracycline. (B) Cells were cultured as described for panel A in the absence or presence of tetracycline for 3 days and then stained with PI, and DNA contents were analyzed by flow cytometry (*x* axis, relative intensity of fluorescence; *y* axis, relative cell number). (C) Cells treated as described for panel B were stained with FITC-annexin V and analyzed.

Microarray data accession numbers. Microarray data have been deposited in the Gene Expression Omnibus database GEO (www.ncbi.nlm.nih.gov/geo) (accession numbers GSE8665 and GSE8596).

RESULTS

EWS/ETS expression results in morphological changes in UET-13 cells. To investigate how the expression of EWS/ETS affects human MPCs, we used UET-13 cells as a model of human MPCs and expressed EWS/FLI1 (UET-13TR-EWS/FLI1) and EWS/ERG (UET-13TR-EWS/ERG) in a tetracycline-inducible manner (Fig. 1A). As shown in Fig. 1B and C, we confirmed that the tetracycline treatment could induce EWS/ETS expression by RT-PCR analysis and Western blotting. The inducibility upon the addition of doxycycline was comparable to that upon the addition of tetracycline.

Using these cell systems, first we examined the effect of EWS/ETS expression on morphology in UET-13 transfectants. When tetracycline was added to the culture, the morphologies of both UET-13TR-EWS/FLI1 and UET-13TR-EWS/ERG cells were dramatically changed (Fig. 1D). Tetracycline-treated UET-13TR-EWS/ETS cells consisted of a mixture of small round-to-polygonal cells and short spindle cells. The cell morphology resembled that of EFT cell lines. To assess the reproducibility of this phenotypic change, other UET-13TR-EWS/ETS clones were examined, and similar morphological changes were observed. Since tetracycline treatment did not affect the morphology of UET-13TR cells (Fig. 1D), it was suggested that the morphological alteration in UET-13 cells from a mesenchymal cell shape to small round cells, one of the characteristics of EFT, can be attributed to EWS/ETS expression.

EWS/ETS expression inhibits cell growth in UET-13 cells. Next, the effect of EWS/ETS expression on the growth of UET-13 cells was analyzed. As shown in Fig. 2A, an MTT assay revealed that the addition of tetracycline had no effect on the growth of UET-13TR cells but slightly inhibited that of UET-13TR-EWS/ETS cells. We also assessed the cell growth of UET-13 transfectants after tetracycline addition by cell counting and obtained results well in accord with those from the MTT assay (data not shown). To determine the mechanism of this inhibition, DNA content and the binding of annexin V to UET-13 transfectants were examined. No significant increase in either sub-G_1-phase cells (Fig. 2B) or annexin V binding cells (Fig. 2C) was detected, suggesting that EWS/ETS-mediated growth inhibition in UET-13 cells was not due to the activation of an apoptotic pathway. Moreover, no significant decrease in S-G_2-phase cells was observed (Fig. 2B).

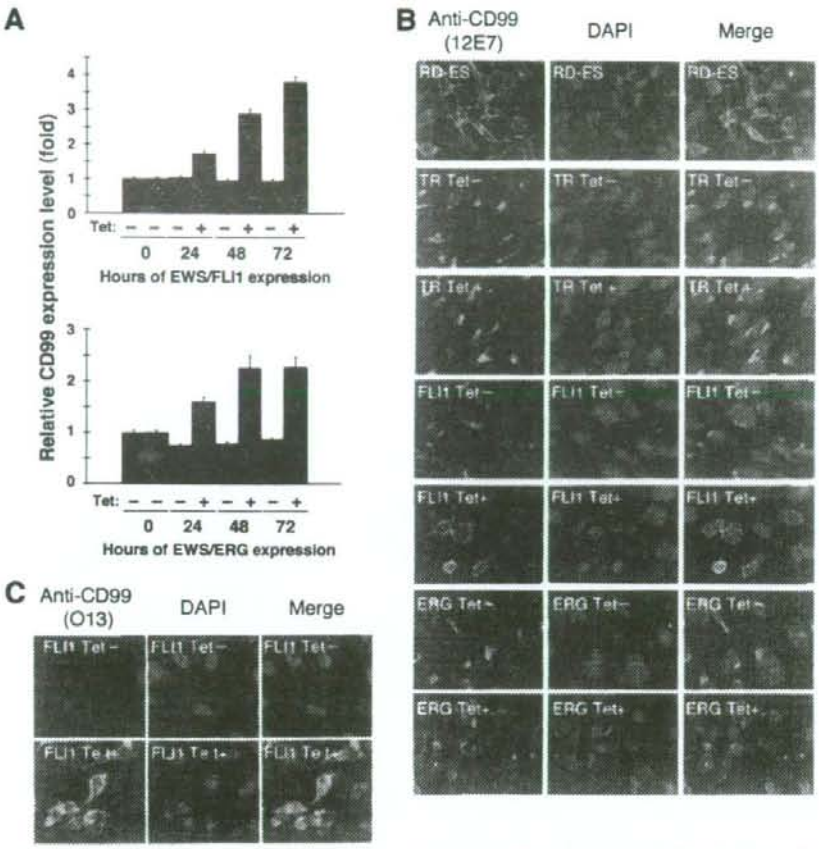

FIG. 3. Effects of tetracycline-mediated EWS/ETS expression on the expression and distribution of CD99 in UET-13 cells. (A) Relative CD99 levels in UET-13 transfectants in the absence or presence of tetracycline (Tet). UET-13 transfectants were treated with or without 3 μg/ml of tetracycline for the indicated periods. Real-time RT-PCR was performed to investigate the expression pattern of CD99. Signal intensities of CD99 were normalized using those of a control housekeeping gene (human GAPDH gene). Data are relative values with standard deviations from triplicate wells and are normalized to the mRNA level at 0 h, which is arbitrarily set to 1 in the graphical presentation. (B and C) Immunocytostaining of CD99 in UET-13 transfectants. Cells were cultured on coverslips in the absence or presence of tetracycline for 72 h and then stained with anti-CD99 antibody 12E7 (B) or O13 (C) as described in Materials and Methods. RD-ES cells were also examined as a positive control. For the staining of nuclei, DAPI was used.

Effect of EWS/ETS on CD99 expression in UET-13 cells. The p30/32MIC-2 gene product, CD99, is a cell surface glycoprotein expressed in EFT with a strong membranous staining pattern and thus constitutes a useful marker for EFT (2, 30). Knowing the dramatic change of morphology in UET-13 cells, we next investigated the mRNA level of CD99 in tetracycline-treated and untreated UET-13 transfectants by quantitative real-time RT-PCR. CD99 levels were clearly elevated by tetracycline treatment in both UET-13TR-EWS/FLI1 and UET-13TR-EWS/ERG cells in a time-dependent manner (Fig. 3A).

We also examined the protein expression of CD99 by immunostaining using 12E7 antibody, which is most widely used as an anti-CD99 antibody. An EFT cell line, RD-ES, showed strong membranous staining of CD99 (Fig. 3B), while neither UET-13TR cells nor UET-13 cells had such a staining. Of note is the fact that although 12E7 reactivity was observed only in the cytoplasm in perinuclear regions in both UET-13TR (Fig. 3B) and UET-13 (data not shown) cells, this antibody is well known to cross-react with a cytoplasmic protein not yet characterized. Since another anti-CD99 antibody, O13, did not react with either UET-13TR (Fig. 3C) or UET-13 (data not shown) cells, we concluded that the perinuclear staining of 12E7 mentioned above was a cross-reaction with unrelated proteins.

In the absence of tetracycline, both UET-13TR-EWS/FLI1 and UET-13TR-EWS/ERG cells were also negative with anti-CD99 antibodies (a pattern designated $CD99^-$), similar to UET-13 cells. Surprisingly, however, tetracycline induced a membranous staining pattern (designated $CD99^+$) in UET-13TR-EWS/FLI1 and UET-13TR-EWS/ERG cells, and some $CD99^+$ cells had irregularly contoured nuclei (Fig. 3B). The same results were observed with another anti-CD99 antibody, O13 (Fig. 3C), indicating that the membranous staining observed for UET-13 transfectants with the anti-CD99 antibodies

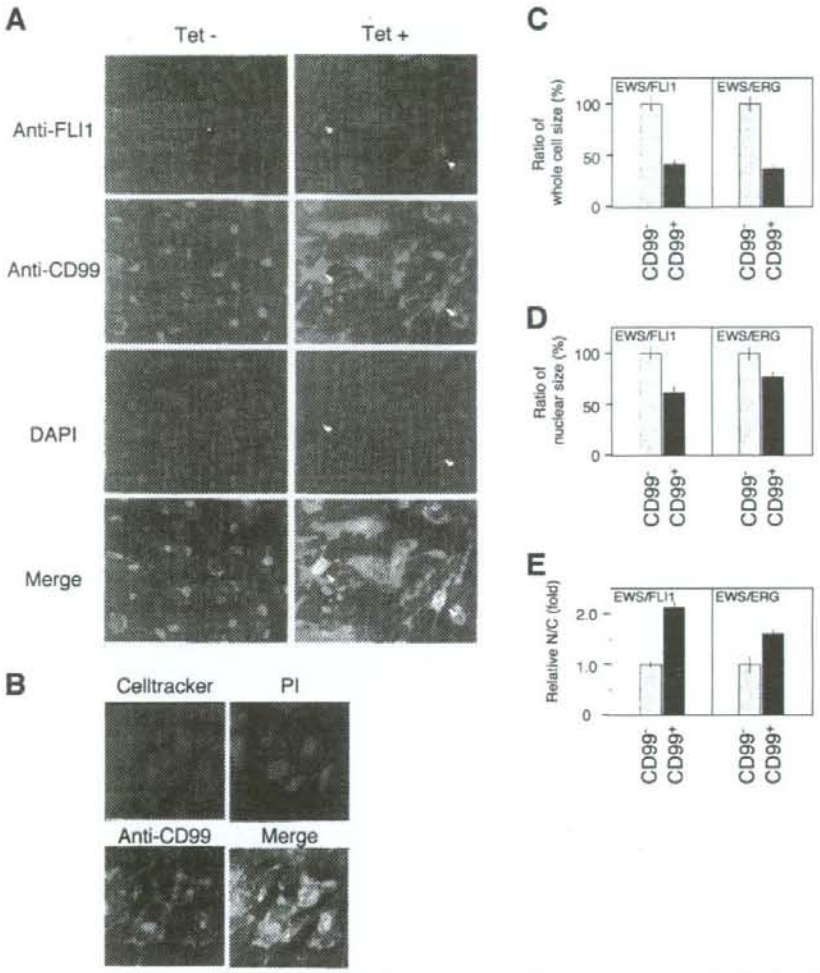

FIG. 4. EWS/ETS expression, alteration of CD99 distribution, and cell morphological changes in UET-13 cells. (A) Immunofluorescence studies using anti-Fli1 (red), anti-CD99 (green), and DAPI (blue). UET-13TR-EWS/FLI1 cells were cultured on coverslips in the absence or presence of tetracycline (Tet) for 72 h and then stained as described in Materials and Methods. White arrowheads indicate $CD99^+$ cells that have a strong staining pattern with anti-Fli1 antibodies and also have remarkable CD99 expression and morphological features. (B) Immunofluorescence analysis by triple staining with whole cells (Celltracker; blue), CD99 (anti-CD99; green), and nuclei (PI; red). UET-13TR-EWS/FLI1 cells were cultured as described for panel A and then stained as described in Materials and Methods. (C to E) Measurements of whole-cell size (C), nuclear size (D), and N/C ratio (E) in tetracycline-treated UET-13 transfectants. UET-13TR-EWS/FLI1 and UET-13TR-EWS/ERG cells were cultured on coverslips in the presence of tetracycline for 72 h and then stained as described in Materials and Methods. These samples were analyzed by the image analysis software Image J ($n = 50$). (C and D) Data are relative values with the SE and are normalized to the size of $CD99^-$ cells, which is arbitrarily set to 100. (E) Data are relative values with the SE and are normalized to the size of $CD99^-$ cells, which is arbitrarily set to 1.

was really CD99 derived. Despite the fact that cells were single colony derived, there was a heterogeneous response to tetracycline treatment in UET-13TR-EWS/FLI1 and UET-13TR-EWS/ERG cells, but most of the $CD99^+$ cells had a small round morphology, one of the characteristics of EFT. To assess the correlation between EWS/FLI1 expression and the change of the CD99 expression pattern, we performed immunofluorescence studies using anti-Fli1 and anti-CD99 antibodies. As shown in Fig. 4A, tetracycline treatment induced a marked enhancement of nuclear staining with anti-Fli1 antibodies in a large number of UET-13TR-EWS/FLI1 cells, indicating the induction of EWS/FLI1 proteins. Furthermore, we observed that the cells with a strong signal for Fli1 tended to reveal a membranous staining pattern with anti-CD99 antibodies and a small round morphology (Fig. 4A). To further verify the correlation between CD99 expression pattern and cell morphology, we estimated the size of cells by triple staining using Celltracker Blue, PI, and anti-CD99 antibody (Fig. 4B). As

TABLE 2. Immunophenotypic characterization of UET-13 transfectants and EFT cells

MPC status[a]	CD marker	Result for[b]: UET-13	UET-13TR		UET-13TR-EWS/FLI1		UET-13TR-EWS/ERG		RD-ES	EFT status[c]	SK-ES1
		Tet$^-$	Tet$^+$	Tet$^-$	Tet$^+$	Tet$^-$	Tet$^+$				
M+	CD29	+	+	+	+	+	+	+	+	+	
M+	CD59	+	+	+	+	+	+	+	+	+	
M+	CD90	+	+	+	+	+	+	+	+	+	E+
M+	CD105	+	+	+	+	+	+	+	+	+	
M+	CD166	+	+	+	+	+	+	+	+	+	
M+	CD44	+	+	+	+	+	+	+	−	−	
M+	CD73	+	+	+	+	+	+	+	−	−	
M+	**CD10**	+	+	+	+	**Down**	+	**Down**	−	−	
M+	**CD13**	+	+	+	+	**Down**	+	**Down**	−	−	
M+	**CD49e**	+	+	+	+	**Down**	+	**Down**	+	−	
M+	**CD61**	+	+	+	+	**Down**	+	**Down**	−	−	
M+	**CD55**	+	+	+	+	**Down**	+	+	+	−	
M+	**CD54**	−	−	−	−	**Up**	−	**Up**	+	+	E+
M(−)	**CD117**	−	−	−	−	**Up**	−	**Up**	+	+	E+
M+/−	**CD271**	−	−	−	−	**Up**	−	**Up**	+	+	E+
	CD40	−	−	−	−	−	−	−	+	+	E+
	CD56	−	−	−	−	−	−	−	+	+	E+
M(−)	CD133	−	−	−	−	−	−	−	+	+	
M(−)	CD14	−	−	−	−	−	−	−	−	−	
M(−)	CD34	−	−	−	−	−	−	−	−	−	
M(−)	CD45	−	−	−	−	−	−	−	−	−	

[a] M(−), negative for MPCs; M+/−, positive for BM-derived MPCs but negative after in vitro culture; M+, positive for MPCs.
[b] +, most cells positive; −, negative; Up, up-regulated by tetracycline treatment; Down, down-regulated by tetracycline treatment. Boldface indicates the antigens the immunophenotypes of which were changed in favor of EFT. Tet$^-$, tetracycline negative; Tet$^+$, tetracycline positive.
[c] E+, positive for EFTs.

presented in Fig. 4C and D, the results clearly showed that the majority of CD99$^+$ cells were significantly smaller in both whole-cell size and nuclear size than the CD99$^-$ cells. Moreover, CD99$^+$ cells also had a substantially increased N/C ratio (Fig. 4E). These results indicated that EWS/ETS expression promoted CD99 expression in UET-13 cells, and CD99 expression status is correlated with the degree of morphological change.

EWS/ETS expression altered the immunophenotype of UET-13 cells. Human MPCs reveal a characteristic expression of several surface antigens and can be identified on the basis of the reactivity with a set of monoclonal antibodies against CD antigens (25, 42). On the other hand, some CD antigens are characteristically expressed on EFT cells (17, 28, 33). Using the combinations of these antibodies listed in Table 2, which are useful for the immunodetection of either MPCs or EFT cells, we further examined whether EWS/ETS expression affects the immunophenotype of UET-13 cells and compared its effect with that on the immunophenotype of EFT cell lines (Table 2 and Fig. 5). As shown in Table 2, UET-13 cells express most of the human primary MPCs markers. Some of the antigens expressed in MPCs, namely, CD29, CD59, CD90, CD105, and CD166, were also found to be expressed in EFT cell lines, but others, namely, CD10, CD13, CD44, CD61, and CD73, were not. In contrast, antigens recognized to be present in EFT cells, including CD40, CD56, and CD133, were absent from UET-13 cells. Interestingly, when the effect of tetracycline-mediated EWS/ETS expression on the immunophenotype of UET-13 cells was tested, levels of some of the antigens present in UET-13 cells, such as CD10, CD13, and CD61, were found to be decreased (Fig. 5). In contrast, some of the markers found in EFT cells, i.e., CD54, CD117, and CD271, became positive in UET-13TR-EWS/ETS cells after tetracycline treatment. Because UET-13TR cells did not show such immunophenotypic change upon treatment with tetracycline, these results indicated that, at least in part, the immunophenotype of UET-13 cells was changed in favor of EFT in the presence of EWS/ETS.

EWS/ETS in UET-13 cells modulates EFT-like gene expression. To further examine the molecular mechanism of EWS/ETS-dependent cellular modulation in human mesenchymal progenitor background, we performed DNA microarray-based expression profiling using the Affymetrix human genome U133 Plus 2.0 array. As a first step to this approach, we validated our experimental systems by analyzing the sequential changes of known EWS/ETS target genes, i.e., inhibitor of differentiation 2 (ID2) (14, 39), NK2 transcription factor related, locus 2 (NKX2.2) (9, 48), and insulin-like growth factor binding protein 3 (IGFBP3) (41). Consistent with previous reports, levels of ID2 and NKX2.2 increased with the expression of EWS/ETS in a time-dependent manner, whereas the expression level of IGFBP3 decreased (Fig. 6A). Employing the same procedure, we also examined whether the change of surface antigen expression was regulated at the transcriptional level and determined the mRNA expression levels of some surface antigens in UET-13 transfectants with or without tetracycline treatment. In accordance with the results of immunocytometric and immunohistological experiments, the mRNA expression levels of CD10, CD13, CD49e, and CD61 were decreased, while those of CD54, CD99, CD117, and CD271 were markedly increased in tetracycline-treated UET-13TR-EWS/ETS cells (Fig. 6B and C), indicating that the expression of these antigens is

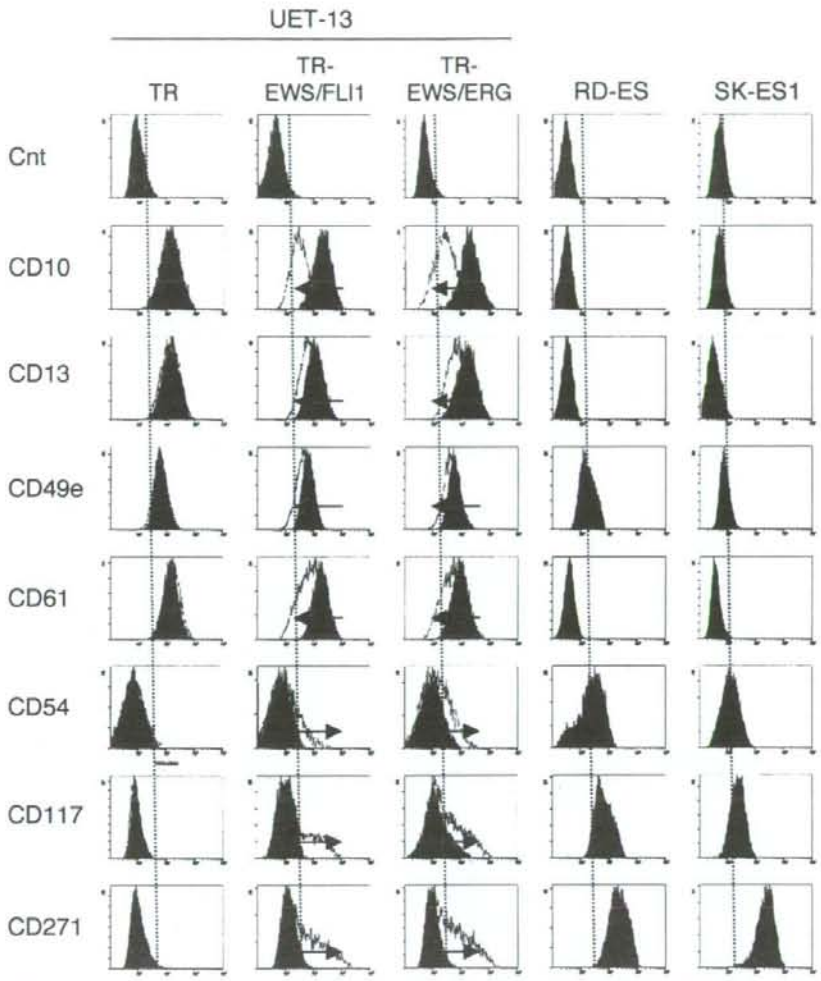

FIG. 5. Immunophenotypic change on induction of EWS/ETS expression in UET-13 cells. UET-13 transfectants were cultured with or without 3 μg/ml of tetracycline for 1 week and flow cytometric analyses were performed by using a set of antibodies as indicated. The histograms of UET-13 transfectants with (empty) and without (gray) tetracycline treatment were overlaid. Dotted lines indicate fluorescence intensities in negative control panels (Cnt). Arrows indicate the immunophenotypic change caused by tetracycline. The immunophenotypes of the EFT cell lines RD-ES and SK-ES1 were also examined.

controlled at the transcriptional level in the presence of EWS/ETS.

We next investigated the candidate genes whose expression is regulated by EWS/ETS in human MPCs. First, we selected the genes with up-regulated or down-regulated expression by EWS/ETS induction using gene cluster analysis (Fig. 7A; UET-13TR-EWS/FLI1 up, 4,294 probes; down, 4,103 probes; UET-13TR-EWS/ERG up, 3,358 probes; down, 3,705 probes). To reduce the number of the candidate genes, we selected up-regulated genes that are expressed in tetracycline-treated cells at least 1.5-fold higher than in untreated cells (UET-13TR-EWS/FLI1, 1,137 probes; UET-13TR-EWS/ERG, 835 probes). Similarly, the down-regulated genes that are expressed in tetracycline-treated cells at least 0.75-fold lower than in untreated cells (UET-13TR-EWS/FLI1, 1,803 probes; UET-13TR-EWS/ERG, 773 probes). By selecting common probes in both cells, we finally identified a group of candidate genes significantly controlled by EWS/ETS induction in the human mesenchymal progenitor background. Since microarray analysis was performed as a global screening in a single experiment, it is likely that there is a fair bit of noise in the derived gene profiles due to the lack of replicate data. This may account in part for the limited overlap between the profiles induced by EWS-FLI1 and EWS-ERG, whereas we still identified 349 probes of common up-regulated genes and 293 probes of common down-regulated genes (see the supplemental material). In addition to the EFT-specific genes mentioned above, these contained those previously described as EFT-specific genes, such as those for OB-cadherin/cadherin-11 (31), Janus

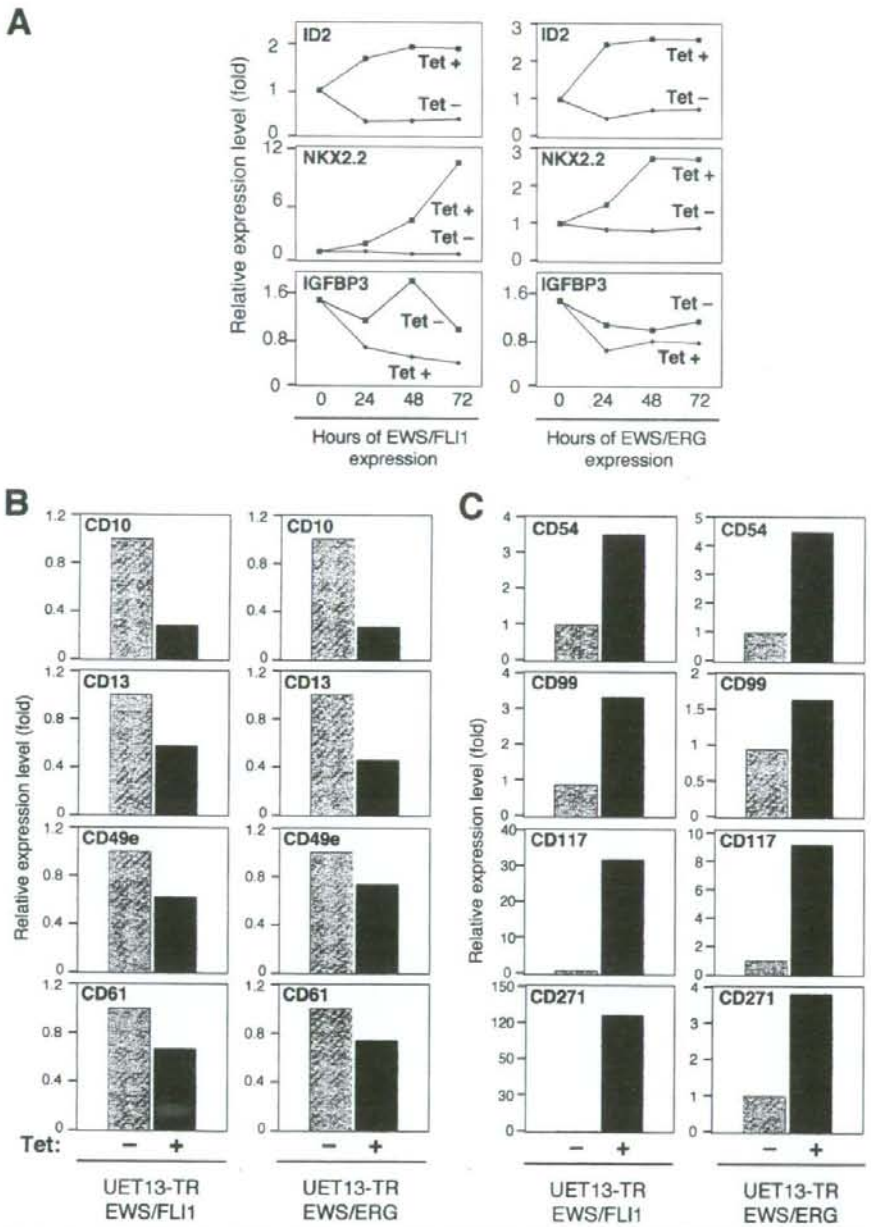

FIG. 6. The change of expression profile on induction of EWS/ETS in UET-13 cells. UET-13TR-EWS/FLI1 and UET-13TR-EWS/ERG cells were cultured in the absence or presence of tetracycline (Tet) for the indicated periods and analyzed using the Affymetrix human genome U133 Plus 2.0 array as described in Materials and Methods. (A) The sequential changes of ID2, NKX2.2, and IGFBP3 mRNA levels in UET-13 transfectants upon treatment with or without tetracycline. Diamond symbols indicate UET-13 transfectants in the absence of tetracycline; box symbols indicate UET-13 transfectants in the presence of tetracycline. (B and C) Microarray studies for the determination of expression profiles of surface antigens in UET-13 transfectants. UET-13 transfectants were treated with or without 3 μg/ml of tetracycline for 72 h. mRNA levels were determined with the Affymetrix human genome U133 Plus 2.0 array.

kinase 1 (JAK1) (49), keratin 18, and six-transmembrane epithelial antigen of the prostate (STEAP) (22). The expression pattern of these genes (642 probes) in UET-13 transfectants in the absence or presence of tetracycline is shown in the gene cluster in Fig. 7B. The expression of these genes was indeed changed significantly after EWS/ETS expression in both cells. They included genes associated with signal transduction (such as those for epidermal growth factor receptor, FAS [CD95], and fibroblast

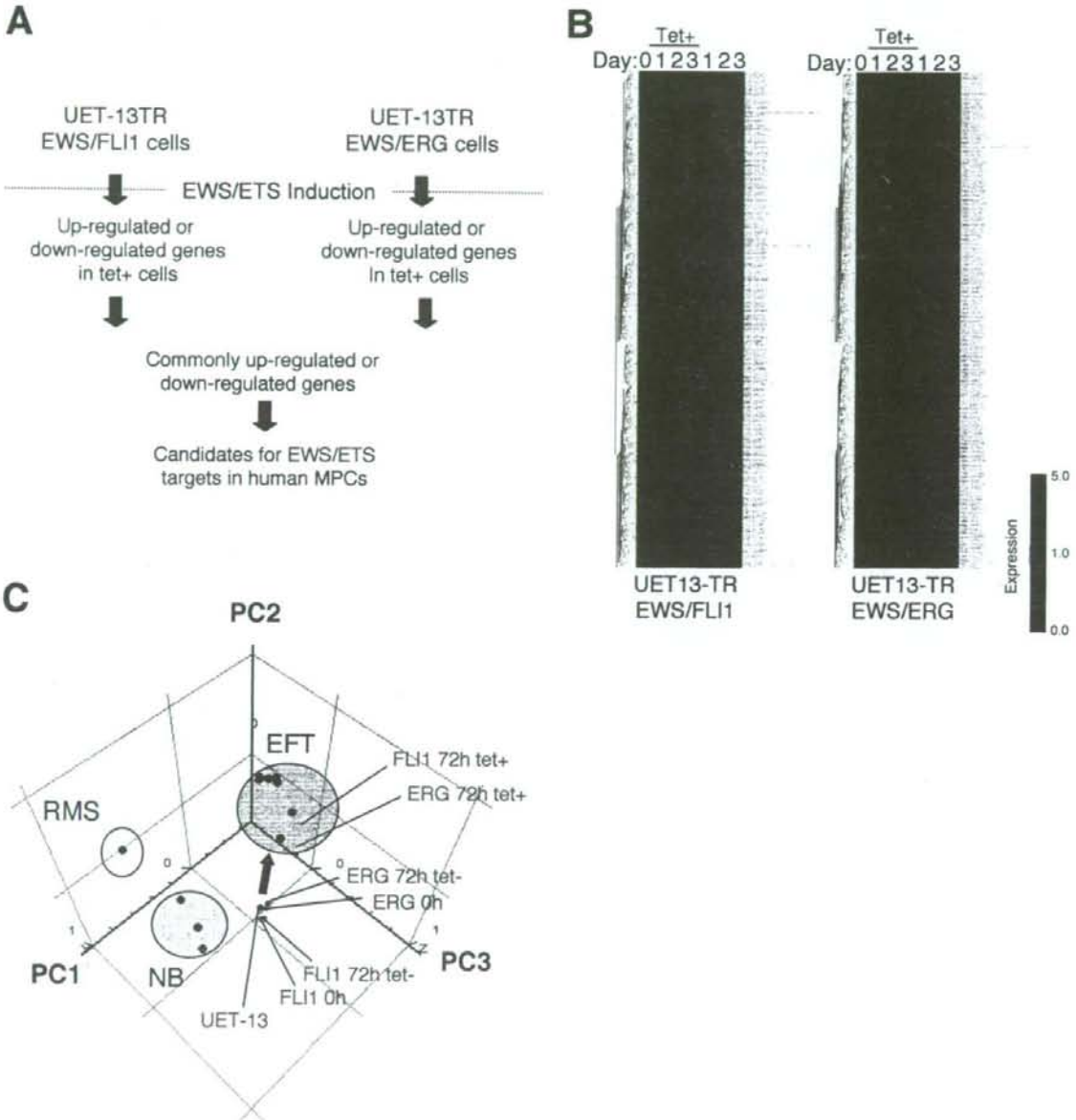

FIG. 7. Identification of candidates for the target of EWS/ETS in human MPCs by use of a microarray. UET-13TR-EWS/FLI1 and UET-13TR-EWS/ERG cells were cultured as described for Fig. 6 and analyzed using the Affymetrix human genome U133 Plus 2.0 array as described in Materials and Methods. (A) Scheme for the analysis of microarray data. (B) Gene cluster analysis of UET-13 transfectants in the absence or presence of tetracycline by use of 642 candidate genes for targets of EWS/ETS in human MPCs. (C) Visualization of sequential change by the gene expression profile in UET-13 transfectants following tetracycline-mediated EWS/ETS expression based on a PCA of 642 candidate genes. Deep blue plots indicate UET-13 cells. Light blue plots indicate UET-13 transfectants in the absence of tetracycline for 72 h. Yellow plots indicate UET-13 transfectants in the presence of tetracycline for 72 h. The pink circle indicates EFT cell lines expressing EWS/FLI1 (purple plots), EWS/ERG (red plot), and EWS/E1AF (light green plot). The light blue circle with blue plots indicates NB cell lines. The yellow circle with an orange plot indicates a rhabdomyosarcoma (RMS) cell line. Cutoff induction and repression levels are 1.5-fold and 0.75-fold, respectively. Tet, tetracycline.

growth factor receptor 1) and development (such as jagged-1 and frizzled-4, -7, and -8). Interestingly, in addition to the surface antigens presented in Fig. 6B and C, the expression profiling of EWS/ETS-expressing UET-13 cells displayed the modulation of several genes associated with cell adhesion, cytoskeletal structure, and membrane trafficking, such as those for collagen-11 and -21, ephrin receptor-A2, -B2, and -B3, ephrin-B1, claudin-1, integrin-α11, -αM, and -β2, CD66 (carcinoembryonic antigen-related cell adhesion molecule-1), and CD102 (intercellular cell adhesion molecule-2). They also included genes of chemokines CCL-2 and -3. These data raise the possibility that EWS/ETS can contribute to the membrane condition in human MPCs via the regulation of these cell surface molecules and chemokines.

Using these genes, we performed a PCA to visualize the shift in the gene expression pattern among the 642 probes. As shown in Fig. 7C, the plots of UET-13 transfectants treated with tetracycline became closer to those of EFT cells than to those of UET-13 transfectants without tetracycline treatment. These results indicated that the expression pattern of these genes was altered from that of UET-13 cells to that of EFT cells in an EWS/ETS-dependent manner. Since the gene expression profile of UET-13 cells is similar to those of other cell types of mesenchymal origin (data not shown), our results highlighted that the phenotypic alteration from mesenchyme to EFT-like cells in UET-13 cells induced by tetracycline treatment was accompanied by a change in the global gene expression profile.

EWS/ETS expression enhances the Matrigel invasion of UET-13 cells. To assess the role of EWS/ETS in malignant transformation in human MPCs, UET-13 transfectants were examined by invasion assay. As shown in Fig. 8A, tetracycline treatment did not affect the Matrigel invasion ability of UET-13TR cells. When examined similarly, however, tetracycline treatment resulted in an apparently increased invasion ($P < 0.05$) for both UET-13TR-EWS/FLI1 (Fig. 8B) and UET-13TR-EWS/ERG (Fig. 8C) cells. The results indicated that EWS/ETS expression can induce Matrigel invasion properties in human MPCs.

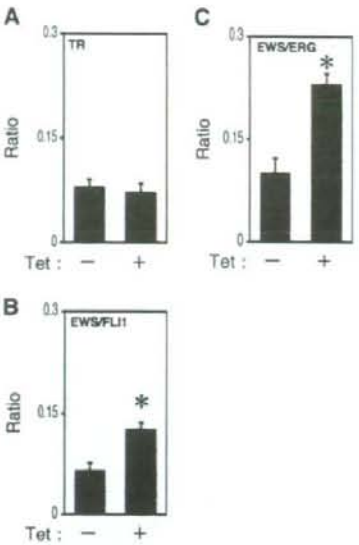

FIG. 8. Effects of EWS/ETS expression on the Matrigel invasion ability of UET-13 cells. UET-13TR (A), UET-13TR-EWS/FLI1 (B), and UET-13TR-EWS/ERG (C) cells were cultured in the absence or presence of tetracycline (Tet) for 72 h and then plated (2.5×10^4) on Matrigel-coated or uncoated filter inserts. After 20 h of culture, invading cells were stained with hematoxylin-eosin and counted in five fields per membrane as described in Materials and Methods. *, $P < 0.05$.

DISCUSSION

In the present study, using UET-13 cells as a model of human MPCs, we demonstrated that ectopic expression of EWS/ETS promoted the acquisition of an EFT-like phenotype, including cellular morphology, immunophenotype, and gene expression profile. Moreover, EWS/ETS expression enhances the ability of UET-13 cells to invade Matrigel. This assay is thought to mimic the early steps of tumor invasion in vivo (34), and the ability to penetrate the Matrigel has been positively correlated with invasion potential in several studies. Therefore, we concluded that EWS/ETS expression could mediate a part of the feature of tumor transformation in human MPCs. Thus, our culture system would provide a good model for testing the effects of EWS/ETS in human MPCs.

Several lines of evidence have indicated the transforming ability of EWS/FLI1, whereas that of EWS/ERG is not yet to be clarified. Therefore, it is noteworthy that our data demonstrated that EWS/ERG could promote an EFT-like phenotype in UET-13 cells similarly to EWS/FLI1. Thus, EWS/ERG also has the ability to induce an EFT-like phenotype in the human system. The major steps in the development of EFT should be commonly regulated by distinct chimeric EWS/ETS proteins. Indeed, several genes are common transcriptional targets of different chimeric EWS/ETS proteins in the murine system (11, 24, 35). Our data also showed that the 642 probes are coregulated in both EWS/FLI1-expressing cells and EWS/ERG-expressing cells. Further comparative studies of both the EWS/FLI1- and the EWS/ERG-mediated onset of EFT could allow us to understand the common functions of EWS/FLI1 and EWS/ERG in EFT. In addition, our systems are also useful for precisely distinguishing between the functions of these chimeric molecules in the development of EFT.

As mentioned above, the immunophenotypic analysis also revealed that the expression profiles of surface antigens in UET-13 cells were changed in favor of EFT cells in the presence of EWS/ETS (Fig. 4). Notably, the expression of CD54 (intercellular cell adhesion molecule-1 [ICAM1]), CD117 (c-kit), and CD271 (low-affinity nerve growth factor receptor [LNGFR]) increased in EWS/ETS-expressing UET-13 cells. These markers are positive in EFT cell lines (17, 28, 33), and in addition, CD117 is detected in about 40% of patient samples (17) and is negative in human primary MPCs (4, 43). Thus, it is reasonable to consider that a phenotypic marker of EFT was induced in UET-13 cells by EWS/ETS expression. On the other hand, CD54 and CD271 are positive in human primary MPCs (8, 25, 42), whereas these markers are negative in UET-13 cells. However, a previous report showed the disappearance of some positive markers, including CD271, from primary human MPCs during the process of ex vivo expansion

(25), and it has been speculated that the expression of these molecules in MPCs is induced in vivo via interaction with the bone marrow microenvironment and that the necessary stimuli are absent from ex vivo culture conditions. Therefore, the immunophenotype of UET-13 cells rather might be related to that of ex vivo-expanded primary human MPCs. In addition, it may be possible that EWS/ETS expression led to the reexpression of these disappeared markers in UET-13 cells without the necessary stimuli. In this case, the maintenance of CD271 expression outside of the bone marrow microenvironment might be a characteristic of EFT. Thus, our results proved that both EWS/FLI1 and EWS/ERG can be major causes of the expression of these markers and that human MPCs that precisely recapitulate the expression are strong candidates for the cell origins of EFT cells. The findings also imply that these antigens are suitable targets for diagnostic tools and new therapeutic agents. In fact, imatinib mesylate, which demonstrates anticancer activity against malignant cells expressing BCR-ABL as well as CD117 and platelet-derived growth factor receptor, inhibits proliferation and increases sensitivity to vincristine and doxorubicin in EFT cells (17).

Notably, our results also indicate that UET-13 cells, which have the MPC phenotype, possess the potential to acquire an EFT-like phenotype upon the expression of EWS/ETS. Unlike what is seen for human primary fibroblasts (31), ectopic EWS/ETS expression induces an EFT-like morphological change in human MPCs, suggesting that the cell type affects susceptibility to the events following EWS/ETS expression. In murine MPCs, retrovirally transduced EWS/FLI1 has been reported to induce the expression of CD99, a most useful marker for EFT, though the results are controversial (6, 45). However, our direct evidence obtained with UET-13 cells clearly demonstrated that CD99 expression is induced by EWS/ETS proteins in human MPCs. Moreover, we showed that the expression of CD99 might correlate with EWS/ETS-mediated morphological change, whereas the functional role of CD99 and the correlation between CD99 expression status and EWS/ETS-mediated morphological change in the development of EFT remain unclarified.

Consistent with the morphological and immunophenotypic changes, the expression pattern of a set of genes in EWS/ETS-expressing UET-13 cells shifted to that in EFT cells (Fig. 7C). Although EWS/ETS expression enhanced the ability of UET-13 cells to invade Matrigel, it did not promote migratory ability and surface-independent growth, as assessed by migration assay and soft agar colony formation assay (data not shown). We also failed to develop EFT-like tumors by injecting EWS/ETS-inducing UET-13 cells into irradiated nude mice treated with tetracycline (data not shown). These results imply that EWS/ETS expression is not sufficient to induce the full transformation in UET-13 cells, and other genetic abnormalities not regulated by EWS/ETS could still be required for the full transformation of human MPCs into EFT cells. An identification of these genes will greatly improve our understanding of the additional genetic lesions that occur after EWS/ETS expression. The genes expressed in EFT cell lines but not in EWS/ETS-expressing UET-13 cells would be candidates for such genes.

In summary, we reported the development of an inducible EWS/ETS expression system in UET-13 cells as a model for the development of EFT in MPCs. In our system, the chimeric genes alone are sufficient to confer EFT-like phenotypes, EFT-specific gene expression pattern, and partial but not full features of malignant transformation. Further analysis using our system should elucidate the pathogenic mechanism by which EFTs develop from MPCs, especially the initiating events mediated by EWS/ETS expression. Our system should also aid in the identification of novel targets of the EWS/ETS-mediated pathway as potential anticancer targets.

ACKNOWLEDGMENTS

This work was supported in part by health and labor sciences research grants (the 3rd-Term Comprehensive 10-Year Strategy for Cancer Control [H19-010], Research on Children and Families [H18-005 and H19-003], Research on Human Genome Tailor Made, and Research on Publicly Essential Drugs and Medical Devices [H18-005]) and a grant for child health and development from the Ministry of Health, Labor and Welfare of Japan, JSPS (Kakenhi 18790263). This work was also supported by a CREST, JST grant from the Japan Health Sciences Foundation for Research on Publicly Essential Drugs and Medical Devices and the Budget for Nuclear Research of the Ministry of Education, Culture, Sports, Science and Technology, based on screening and counseling by the Atomic Energy Commission. Y. Miyagawa is an awardee of a research resident fellowship from the Foundation for Promotion of Cancer Research (Japan) for the 3rd-Term Comprehensive 10-Year Strategy for Cancer Control.

We are grateful to T. Motoyama for the NRS-1 cell line. We respectfully thank S. Yamauchi for her secretarial work and M. Itagaki for many helpful discussions and support.

REFERENCES

1. **Akagi, T.** 2004. Oncogenic transformation of human cells: shortcomings of rodent model systems. Trends Mol. Med. **10**:542–548.
2. **Ambros, I. M., P. F. Ambros, S. Strehl, H. Kovar, H. Gadner, and M. Salzer-Kuntschik.** 1991. MIC2 is a specific marker for Ewing's sarcoma and peripheral primitive neuroectodermal tumors. Evidence for a common histogenesis of Ewing's sarcoma and peripheral primitive neuroectodermal tumors from MIC2 expression and specific chromosome aberration. Cancer **67**:1886–1893.
3. **Arvand, A., and C. T. Denny.** 2001. Biology of EWS/ETS fusions in Ewing's family tumors. Oncogene **20**:5747–5754.
4. **Bertani, N., P. Malatesta, G. Volpi, P. Sonego, and R. Perris.** 2005. Neurogenic potential of human mesenchymal stem cells revisited: analysis by immunostaining, time-lapse video and microarray. J. Cell Sci. **118**:3925–3936.
5. **Bloom, E. T.** 1972. Further definition by cytotoxicity tests of cell surface antigens of human sarcomas in culture. Cancer Res. **32**:960–967.
6. **Castillero-Trejo, Y., S. Eliazer, L. Xiang, J. A. Richardson, and R. L. Ilaria, Jr.** 2005. Expression of the EWS/FLI-1 oncogene in murine primary bone-derived cells results in EWS/FLI-1-dependent, Ewing sarcoma-like tumors. Cancer Res. **65**:8698–8705.
7. **Colter, D. C., I. Sekiya, and D. J. Prockop.** 2001. Identification of a subpopulation of rapidly self-renewing and multipotential adult stem cells in colonies of human marrow stromal cells. Proc. Natl. Acad. Sci. USA **98**: 7841–7845.
8. **Conget, P. A., and J. J. Minguell.** 1999. Phenotypical and functional properties of human bone marrow mesenchymal progenitor cells. J. Cell. Physiol. **181**:67–73.
9. **Davis, S., and P. S. Meltzer.** 2006. Ewing's sarcoma: general insights from a rare model. Cancer Cell **9**:331–332.
10. **Deneen, B., and C. T. Denny.** 2001. Loss of p16 pathways stabilizes EWS/FLI1 expression and complements EWS/FLI1 mediated transformation. Oncogene **20**:6731–6741.
11. **Deneen, B., S. M. Welford, T. Ho, F. Hernandez, I. Kurland, and C. T. Denny.** 2003. PIM3 proto-oncogene kinase is a common transcriptional target of divergent EWS/ETS oncoproteins. Mol. Cell. Biol. **23**:3897–3908.
12. **Eliazer, S., J. Spencer, D. Ye, E. Olson, and R. L. Ilaria, Jr.** 2003. Alteration of mesodermal cell differentiation by EWS/FLI-1, the oncogene implicated in Ewing's sarcoma. Mol. Cell. Biol. **23**:482–492.
13. **Fujii, Y., Y. Nakagawa, T. Hongo, Y. Igarashi, Y. Naito, and M. Maeda.** 1989. Cell line of small round cell tumor originating in the chest wall: W-ES. Hum. Cell **2**:190–191. (In Japanese.)
14. **Fukuma, M., H. Okita, J. Hata, and A. Umezawa.** 2003. Upregulation of Id2, an oncogenic helix-loop-helix protein, is mediated by the chimeric EWS/ets protein in Ewing sarcoma. Oncogene **22**:1–9.
15. **Gilbert, F., G. Balaban, P. Moorhead, D. Bianchi, and H. Schlesinger.** 1982.

Abnormalities of chromosome 1p in human neuroblastoma tumors and cell lines. Cancer Genet. Cytogenet. 7:33–42.
16. **Girish, V., and A. Vijayalakshmi.** 2004. Affordable image analysis using NIH Image/ImageJ. Indian J. Cancer 41:47.
17. **Gonzalez, I., E. J. Andreu, A. Panizo, S. Inoges, A. Fontalba, J. L. Fernandez-Luna, M. Gaboli, L. Sierrasesumaga, S. Martin-Algarra, J. Pardo, F. Prosper, and E. de Alava.** 2004. Imatinib inhibits proliferation of Ewing tumor cells mediated by the stem cell factor/KIT receptor pathway, and sensitizes cells to vincristine and doxorubicin-induced apoptosis. Clin. Cancer Res. 10:751–761.
18. **Hansen, M. B., S. E. Nielsen, and K. Berg.** 1989. Re-examination and further development of a precise and rapid dye method for measuring cell growth/cell kill. J. Immunol. Methods 119:203–210.
19. **Hara, S., E. Ishii, S. Tanaka, J. Yokoyama, K. Katsumata, J. Fujimoto, and J. Hata.** 1989. A monoclonal antibody specifically reactive with Ewing's sarcoma. Br J. Cancer 60:875–879.
20. **Hatori, M., H. Doi, M. Watanabe, H. Sasano, M. Hosaka, S. Kotajima, F. Urano, J. Hata, and S. Kokubun.** 2006. Establishment and characterization of a clonal human extraskeletal Ewing's sarcoma cell line, EES1. Tohoku J. Exp. Med. 210:221–230.
21. **Homma, C., Y. Kaneko, K. Sekine, S. Hara, J. Hata, and M. Sakurai.** 1989. Establishment and characterization of a small round cell sarcoma cell line, SCCH-196, with t(11;22)(q24;q12). Jpn. J. Cancer Res. 80:861–865.
22. **Hubert, R. S., I. Vivanco, E. Chen, S. Rastegar, K. Leong, S. C. Mitchell, R. Madraswala, Y. Zhou, J. Kuo, A. B. Raitano, A. Jakobovits, D. C. Saffran, and D. E. Afar.** 1999. STEAP: a prostate-specific cell-surface antigen highly expressed in human prostate tumors. Proc. Natl. Acad. Sci. USA 96:14523–14528.
23. **Hu-Lieskovan, S., J. Zhang, L. Wu, H. Shimada, D. E. Schofield, and T. J. Triche.** 2005. EWS-FLI1 fusion protein up-regulates critical genes in neural crest development and is responsible for the observed phenotype of Ewing's family of tumors. Cancer Res. 65:4633–4644.
24. **Im, Y. H., H. T. Kim, C. Lee, D. Poulin, S. Welford, P. H. Sorensen, C. T. Denny, and S. J. Kim.** 2000. EWS-FLI1, EWS-ERG, and EWS-ETV1 oncoproteins of Ewing tumor family all suppress transcription of transforming growth factor beta type II receptor gene. Cancer Res. 60:1536–1540.
25. **Jones, E. A., S. E. Kinsey, A. English, R. A. Jones, L. Straszynski, D. M. Meredith, A. F. Markham, A. Jack, P. Emery, and D. McGonagle.** 2002. Isolation and characterization of bone marrow multipotential mesenchymal progenitor cells. Arthritis Rheum. 46:3349–3360.
26. **Khoury, J. D.** 2005. Ewing sarcoma family of tumors. Adv. Anat. Pathol. 12:212–220.
27. **Kiyokawa, N., Y. Kokai, K. Ishimoto, H. Fujita, J. Fujimoto, and J. L. Hata.** 1990. Characterization of the common acute lymphoblastic leukaemia antigen (CD10) as an activation molecule on mature human B cells. Clin. Exp. Immunol. 79:322–327.
28. **Konemann, S., T. Bolling, A. Schuck, J. Malath, A. Kolkmeyer, K. Horn, D. Riesenbeck, S. Hesselmann, R. Diallo, J. Vormoor, and N. A. Willich.** 2003. Effect of radiation on Ewing tumour subpopulations characterized on a single-cell level: intracellular cytokine, immunophenotypic, DNA and apoptotic profile. Int. J. Radiat. Biol. 79:181–192.
29. **Kovar, H., and A. Bernard.** 2006. CD99-positive "Ewing's sarcoma" from mouse bone marrow-derived mesenchymal progenitor cells? Cancer Res. 66:9786.
30. **Kovar, H., M. Dworzak, S. Strehl, E. Schnell, I. M. Ambros, P. F. Ambros, and H. Gadner.** 1990. Overexpression of the pseudoautosomal gene MIC2 in Ewing's sarcoma and peripheral primitive neuroectodermal tumor. Oncogene 5:1067–1070.
31. **Lessnick, S. L., C. S. Dacwag, and T. R. Golub.** 2002. The Ewing's sarcoma oncoprotein EWS/FLI induces a p53-dependent growth arrest in primary human fibroblasts. Cancer Cell 1:393–401.
32. **Lin, P. P., R. I. Brody, A. C. Hamelin, J. E. Bradner, J. H. Healey, and M. Ladanyi.** 1999. Differential transactivation by alternative EWS-FLI1 fusion proteins correlates with clinical heterogeneity in Ewing's sarcoma. Cancer Res. 59:1428–1432.
33. **Lipinski, M., K. Braham, I. Philip, J. Wiels, T. Philip, C. Goridis, G. M. Lenoir, and T. Tursz.** 1987. Neuroectoderm-associated antigens on Ewing's sarcoma cell lines. Cancer Res. 47:183–187.
34. **Lochter, A., A. Srebrow, C. J. Sympson, N. Terracio, Z. Werb, and M. J. Bissell.** 1997. Misregulation of stromelysin-1 expression in mouse mammary tumor cells accompanies acquisition of stromelysin-1-dependent invasive properties. J. Biol. Chem. 272:5007–5015.
35. **May, W. A., A. Arvand, A. D. Thompson, B. S. Braun, M. Wright, and C. T. Denny.** 1997. EWS/FLI1-induced manic fringe renders NIH 3T3 cells tumorigenic. Nat. Genet. 17:495–497.
36. **May, W. A., S. L. Lessnick, B. S. Braun, M. Klemsz, B. C. Lewis, L. B. Lunsford, R. Hromas, and C. T. Denny.** 1993. The Ewing's sarcoma EWS/FLI-1 fusion gene encodes a more potent transcriptional activator and is a more powerful transforming gene than FLI-1. Mol. Cell. Biol. 13:7393–7398.
37. **Miyagawa, Y., J. M. Lee, T. Maeda, K. Koga, Y. Kawaguchi, and T. Kusakabe.** 2005. Differential expression of a Bombyx mori AHA1 homologue during spermatogenesis. Insect Mol. Biol. 14:245–253.
38. **Mori, T., T. Kiyono, H. Imabayashi, Y. Takeda, K. Tsuchiya, S. Miyoshi, H. Makino, K. Matsumoto, H. Saito, S. Ogawa, M. Sakamoto, J. Hata, and A. Umezawa.** 2005. Combination of hTERT and bmi-1, E6, or E7 induces prolongation of the life span of bone marrow stromal cells from an elderly donor without affecting their neurogenic potential. Mol. Cell. Biol. 25:5183–5195.
39. **Nishimori, H., Y. Sasaki, K. Yoshida, H. Irifune, H. Zembutsu, T. Tanaka, T. Aoyama, T. Hosaka, S. Kawaguchi, T. Wada, J. Hata, J. Toguchida, Y. Nakamura, and T. Tokino.** 2002. The Id2 gene is a novel target of transcriptional activation by EWS-ETS fusion proteins in Ewing family tumors. Oncogene 21:8302–8309.
40. **Ogose, A., T. Motoyama, T. Hotta, and H. Watanabe.** 1995. In vitro differentiation and proliferation in a newly established human rhabdomyosarcoma cell line. Virchows Arch. 426:385–391.
41. **Prieur, A., F. Tirode, P. Cohen, and O. Delattre.** 2004. EWS/FLI-1 silencing and gene profiling of Ewing cells reveal downstream oncogenic pathways and a crucial role for repression of insulin-like growth factor binding protein 3. Mol. Cell. Biol. 24:7275–7283.
42. **Quirici, N., D. Soligo, P. Bossolasco, F. Servida, C. Lumini, and G. L. Deliliers.** 2002. Isolation of bone marrow mesenchymal stem cells by anti-nerve growth factor receptor antibodies. Exp. Hematol. 30:783–791.
43. **Reyes, M., T. Lund, T. Lenvik, D. Aguiar, L. Koodie, and C. M. Verfaillie.** 2001. Purification and ex vivo expansion of postnatal human marrow mesodermal progenitor cells. Blood 98:2615–2625.
44. **Reyes, M., and C. M. Verfaillie.** 2001. Characterization of multipotent adult progenitor cells, a subpopulation of mesenchymal stem cells. Ann. N. Y. Acad. Sci. 938:231–235.
45. **Riggi, N., L. Cironi, P. Provero, M. L. Suva, K. Kaloulis, C. Garcia-Echeverria, F. Hoffmann, A. Trumpp, and I. Stamenkovic.** 2005. Development of Ewing's sarcoma from primary bone marrow-derived mesenchymal progenitor cells. Cancer Res. 65:11459–11468.
46. **Riggi, N., M. L. Suva, and I. Stamenkovic.** 2006. Ewing's sarcoma-like tumors originate from EWS-FLI-1-expressing mesenchymal progenitor cells. Cancer Res. 66:9786.
47. **Sekiguchi, M., T. Oota, K. Sakakibara, N. Inui, and G. Fujii.** 1979. Establishment and characterization of a human neuroblastoma cell line in tissue culture. Jpn. J. Exp. Med. 49:67–83.
48. **Smith, R., L. A. Owen, D. J. Trem, J. S. Wong, J. S. Whangbo, T. R. Golub, and S. L. Lessnick.** 2006. Expression profiling of EWS/FLI identifies NKX2.2 as a critical target gene in Ewing's sarcoma. Cancer Cell 9:405–416.
49. **Staege, M. S., C. Hutter, I. Neumann, S. Foja, U. E. Hattenhorst, G. Hansen, D. Afar, and S. E. Burdach.** 2004. DNA microarrays reveal relationship of Ewing family tumors to both endothelial and fetal neural crest-derived cells and define novel targets. Cancer Res. 64:8213–8221.
50. **Takeda, Y., T. Mori, H. Imabayashi, T. Kiyono, S. Gojo, S. Miyoshi, N. Hida, M. Ita, K. Segawa, S. Ogawa, M. Sakamoto, S. Nakamura, and A. Umezawa.** 2004. Can the life span of human marrow stromal cells be prolonged by bmi-1, E6, E7, and/or telomerase without affecting cardiomyogenic differentiation? J. Gene Med. 6:833–845.
51. **Tondreau, T., N. Meuleman, A. Delforge, M. Dejeneffe, R. Leroy, M. Massy, C. Mortier, D. Bron, and L. Lagneaux.** 2005. Mesenchymal stem cells derived from CD133-positive cells in mobilized peripheral blood and cord blood: proliferation, Oct4 expression, and plasticity. Stem Cells 23:1105–1112.
52. **Torchia, E. C., S. Jaishankar, and S. J. Baker.** 2003. Ewing tumor fusion proteins block the differentiation of pluripotent marrow stromal cells. Cancer Res. 63:3464–3468.
53. **Woodbury, D., E. J. Schwarz, D. J. Prockop, and I. B. Black.** 2000. Adult rat and human bone marrow stromal cells differentiate into neurons. J. Neurosci. Res. 61:364–370.

Immunology
The journal of cells, molecules, systems and technologies
British Society for immunology

IMMUNOLOGY ORIGINAL ARTICLE

B-cell-activating factor inhibits CD20-mediated and B-cell receptor-mediated apoptosis in human B cells

Yohei Saito,[1,2] Yoshitaka Miyagawa,[1] Keiko Onda,[1,2] Hideki Nakajima,[1] Ban Sato,[1] Yasuomi Horiuchi,[1] Hajime Okita,[1] Yohko U. Katagiri,[1] Masahiro Saito,[1,2] Toshiaki Shimizu,[2] Junichiro Fujimoto[1] and Nobutaka Kiyokawa[1]

[1]*Department of Developmental Biology, National Research Institute for Child Health and Development, Setagaya-ku, Tokyo, Japan, and* [2]*Department of Pediatrics, Juntendo University, School of Medicine, Bunkyo-ku, Tokyo, Japan*

doi:10.1111/j.1365-2567.2008.02872.x
Received 22 January 2008; revised 21 April 2008; accepted 30 April 2008.
Correspondence: Dr N. Kiyokawa, Department of Developmental Biology, National Research Institute for Child Health and Development, 2-10-1, Okura, Setagaya-ku, Tokyo 157-8535, Japan.
Email: nkiyokawa@nch.go.jp
Senior author: Nobutaka Kiyokawa

Summary

B-cell-activating factor (BAFF) is a survival and maturation factor for B cells belonging to the tumour necrosis factor superfamily. Among three identified functional receptors, the BAFF receptor (BAFF-R) is thought to be responsible for the effect of BAFF on B cells though details of how remain unclear. We determined that a hairy-cell leukaemia line, MLMA, expressed a relatively high level of BAFF-R and was susceptible to apoptosis mediated by either CD20 or B-cell antigen receptor (BCR). Using MLMA cells as an *in vitro* model of mature B cells, we found that treatment with BAFF could inhibit apoptosis mediated by both CD20 and BCR. We also observed, using immunoblot analysis and microarray analysis, that BAFF treatment induced activation of nuclear factor-κB2 following elevation of the expression level of *Bcl-2*, which may be involved in the molecular mechanism of BAFF-mediated inhibition of apoptosis. Interestingly, BAFF treatment was also found to induce the expression of a series of genes, such as that for CD40, related to cell survival, suggesting the involvement of a multiple mechanism in the BAFF-mediated anti-apoptotic effect. MLMA cells should provide a model for investigating the molecular basis of the effect of BAFF on B cells *in vitro* and will help to elucidate how B cells survive in the immune system in which BAFF-mediated signalling is involved.

Keywords: apoptosis; B-cell-activating factor; Bcl-2; B-cell receptor; CD20

Introduction

The immune system comprises a variety of immune effector cells, including T and B lymphocytes and antigen-presenting cells, such as dendritic cells and others; it protects individuals from infections and cancer. To maintain these sophisticated mechanisms, a very subtle balance between the life and death of the immune effector cells must be maintained to eliminate, by apoptosis, potentially harmful self-reactive lymphocytes and only allow the survival, development and activation of safe and protective immune cells. For this purpose, a number of molecules are involved in this regulatory system.[1]

B-cell-activating factor (BAFF, also termed BlyS, TALL-1, THANK and zTNF4) produced by monocytes, dendritic cells and some T cells is a member of the tumour necrosis factor (TNF) superfamily and is a type 2 transmembrane-bound protein that can also be expressed as a soluble ligand.[2] BAFF was first described as a factor that stimulates cell proliferation and the secretion of immunoglobulin in B cells.[3–7] Transgenic mice that overexpress BAFF in lymphoid tissues exhibited hyperplasia of the mature B-cell compartment.[8–10] In contrast, mice deficient in BAFF showed a deficit in peripheral B lymphocytes[10,11] and an almost complete loss of follicular and marginal zone B lymphocytes in secondary lymphoid organs. This suggests an absolute requirement for BAFF in normal B-cell development.[10] In contrast, a later examination of immunized BAFF-null mice validated the BAFF-independent nature of germinal centre formation and that antibody responses, including high-affinity responses, were attenuated, indicating that BAFF is required for maintenance, but not initiation, of the germinal centre reaction.[12] Based on the above evidence, BAFF is considered to be a survival and maturation factor for B lymphocytes and has emerged as a crucial factor that modulates B-cell tolerance and homeostasis.[2,13] However, the precise role of BAFF in B-cell development is

still controversial and it has been reported that the capacity of B lymphocytes to bind BAFF is correlated with their maturation state and that the effect of BAFF is dependent on the maturation stage of the B lymphocytes.[2,14]

Recent studies have further shown that BAFF affects not only B lymphocytes but also T lymphocytes.[15,16] The three distinct receptors for BAFF, namely the BAFF receptor (BAFF-R, also termed BR3), the B-cell maturation antigen (BCMA), and the transmembrane activator and calcium modulator and cyclophilin ligand interactor (TACI), have been identified and BAFF binds with a similar high affinity to these receptors.[7,17–23] Among these receptors, however, BAFF-R is thought to be responsible for the survival and differentiation of B cells,[24] whereas the molecular basis of BAFF-mediated signalling remains unclear.

A number of systems inducing apoptosis in B cells are present to eliminate inappropriate clones, such as self-acting B cells. For example, it is reported that stimulation via particular surface molecules, including B-cell receptor antigen (BCR) and CD20, induces apoptosis in cultured B cells.[25,26] The balance between apoptosis-inducing systems and survival systems, such as CD20 and BAFF-mediated signalling, would be important for the maintenance of appropriate B-cell development, though details are not known.

To elucidate the molecular basis of the interaction between apoptosis-inducing signals and BAFF-mediated cell survival signals in B cells, we have employed a B-cell line that expresses BAFF-R and is sensitive to CD20-mediated and BCR-mediated apoptosis. In this paper, we present evidence that BAFF-mediated stimulation inhibits the apoptosis induced by both CD20-mediated and BCR-mediated signalling. The possible mechanisms involved in BAFF-mediated cell responses that regulate these apoptotic stimuli are discussed.

Materials and methods

Cells and reagents

The human hairy cell leukaemia cell line MLMA was obtained from the Japanese Cancer Research Resources Bank (JCRB, Tokyo, Japan). Cells were cultured in RPMI-1640 medium supplemented with 10% fetal calf serum at 37° in a humidified 5% CO_2 atmosphere.

Recombinant human BAFF and a proliferation-inducing ligand (APRIL) were obtained from R&D Systems, Inc. (Minneapolis, MN), and used at a concentration of 400 ng/ml for cell stimulation unless otherwise described. The mouse monoclonal antibodies (mAbs) used for the immunofluorescence analysis were anti-CD10, anti-CD20, anti-CD21, anti-CD22, anti-CD24, anti-CD40, anti-human leucocyte antigen DR (HLA-DR; Beckman Coulter, Inc., Fullerton, CA); anti-CD19 (Becton Dickinson and Company, BD, Franklin Lakes, NJ); anti-κ, anti-λ, anti-μ, anti-δ, anti-γ (Dako, Denmark A/S); anti-BAFF-R (Santa Cruz Biotechnology, Santa Cruz, CA); and anti-CD45 (American Type Culture Collection, ATCC, Manassas, VA). The rat mAbs against BCMA (Vicky-1) and TACI (1A1) were purchased from Santa Cruz Biotechnology. The mouse mAbs used for the immunochemical analysis were anti-caspase-2, anti-caspase-3 and anti-glycogen synthase kinase-3β (GSK-3β; Becton Dickinson); anti-caspase-9 (Medical & Biological Laboratories Co., Ltd, Nagoya, Japan); anti-nuclear factor-κB (NF-κB) p52 (C-5), anti-Bcl-2 (100) from Santa Cruz; and anti-β-actin (AC-15) from Sigma-Aldrich Co. (St Louis, MO). The rabbit polyclonal antibodies used were anti-cleaved poly ADP-ribose polymerase (PARP), anti-cleaved caspase-3, anti-phospho-GSK-3β (Ser9) and anti-phospho-GSK-3α/β (Ser9, 21) from Cell Signaling Technology, Inc. (Danvers, MA). A goat anti-NF-κB p50 (C-19) from Santa Cruz was also used. Secondary antibodies, including fluorescein isothiocyanate- (FITC) and enzyme-conjugated antibodies, were purchased from either Jackson ImmunoResearch Laboratories, Inc. (West Grove, PA) or Dako. To cross-link BCR, purified anti-μ rabbit polyclonal antibody (10 μg/ml) from Jackson ImmunoResearch Laboratories, Inc. was used. To cross-link CD20, a mouse anti-CD20 mAb from Beckman Coulter and a secondary anti-mouse immunoglobulin antibody from Jackson ImmunoResearch Laboratories, Inc. were used each at a concentration of 5 μg/ml.

Immunofluorescence analysis and detection of apoptosis

Cells were stained with FITC-labelled mAbs and analysed by flow cytometry (EPICS-XL, Beckman Coulter) as described previously.[27] To quantify the incidence of apoptosis, cells were incubated with FITC-labelled annexin V using a MEBCYTO-Apoptosis kit (Medical & Biological Laboratories Co., Ltd) and then analysed by flow cytometry according to the manufacturer's directions. Apoptotic cells were also detected by nuclear-staining with DAPI and examined by confocal microscopy as described previously.[28] The enzymatic activity of caspases -2, -3, -9 was assessed by using a colorimetric protease assay kit for each caspase (Medical & Biological Laboratories Co., Ltd) according to the manufacturer's protocol.

Immunoblotting

Immunoblotting was performed as described previously.[29] Briefly, cell lysates were prepared by solubilizing the cells in lysis buffer (containing 20 mM Na_2PO_4, pH 7·4, 150 mM NaCl, 1% Triton X-100, 1% aprotinin, 1 mM phenylmethylsulphonylfluoride, 100 mM NaF, and 2 mM Na_3VO_4), and the total protein concentration was determined using a Bio-Rad protein assay kit (Bio-Rad, Hercules, CA). For each cell lysate, 20 μg was separated by

sodium dodecyl sulphate–polyacrylamide gel electrophoresis and transferred to a nitrocellulose membrane using a semidry Transblot system (Bio-Rad). After blocking with 3% skimmed milk in phosphate-buffered saline, the membrane was incubated with the appropriate combination of primary and secondary antibodies as indicated, washed intensively, and examined using the enhanced chemiluminescence reagent system (ECL plus; GE Healthcare Bio-Sciences AB, Uppsala, Sweden).

DNA microarray analysis

The DNA microarray analysis was performed using GeneChip (Affymetrix, Santa Clara, CA). Total RNA isolated from MLMA cells treated with and without BAFF for 12 hr was reverse transcribed and labelled using One-Cycle Target Labeling and Control Reagents as instructed by the manufacturer (Affymetrix). The labelled probes were hybridized to Human Genome U133 Plus 2.0 Arrays (Affymetrix). The arrays were analysed using GeneChip Operating Software 1.2 (Affymetrix). Background subtraction and normalization were performed with GeneSpring GX 7.3 software (Agilent Technologies, Santa Clara, CA). Signal intensities were prenormalized based on the median of all measurements on that chip. To account for the difference in detection efficiency between the spots, prenormalized signal intensities on each gene were normalized to the median of prenormalized measurements for that gene. The data were filtered with the following steps. (1) Genes that were scored as absent in both samples were eliminated. (2) Genes with a signal intensity lower than 90 in both samples were eliminated. (3) Performing cluster analysis using filtering genes, genes were selected that exhibited increased expression or decreased expression in BAFF-treated cells.

Results

Immunophenotypic characterization of MLMA cells

While screening to identify human cell lines expressing BAFF-R, we found that MLMA cells expressed higher levels of BAFF-R than other human B-cell lines. Although the MLMA cell line is known to have been established from a patient with hairy-cell leukaemia, details were not reported. Therefore, we first examined the immunophenotypic characteristics of MLMA cells. Consistent with the JCRB records, flow cytometric analysis revealed that MLMA cells expressed high levels of μ heavy chain and low levels of δ heavy chain with expression of κ light chain (Fig. 1a). In addition to the CD19 and HLA-DR, MLMA cells were found to express mature B-cell

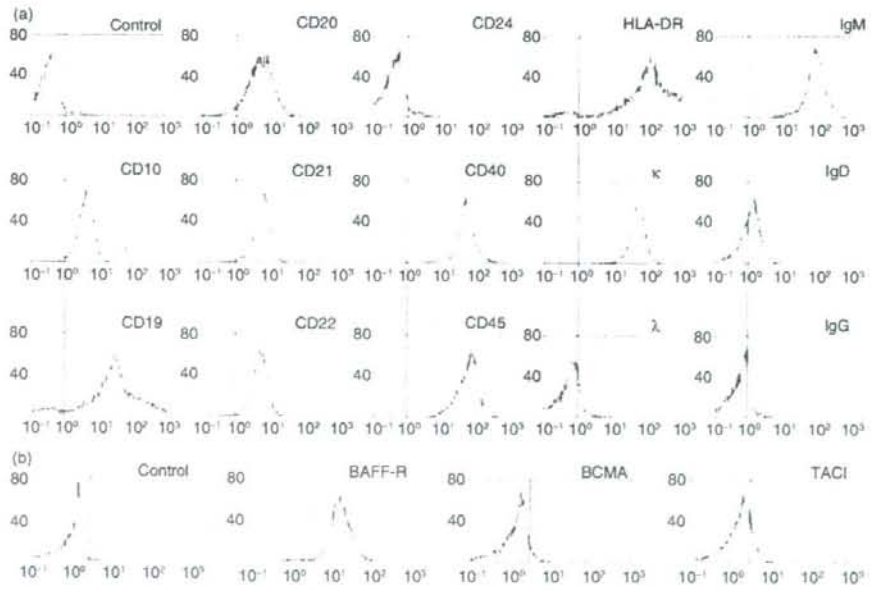

Figure 1. Immunophenotypic characterization of MLMA cells. (a) MLMA cells were stained with specific fluorescein isothiocyanate (FITC)-labelled monoclonal antibodies (mAbs) against B-cell differentiation antigens and analysed by flow cytometry. The *x* axis represents fluorescence intensity and the *y* axis the relative cell number; control was isotype matched mouse immunoglobulin. (b) The expression of B-cell activating factor receptor (BAFF-R), transmembrane activator and calcium modulator and cyclophilin ligand interactor (TACI), and B-cell maturation antigen (BCMA) on MLMA cells was also examined as in (a).

antigens, including CD20, CD21, CD22 and CD40, but not CD24. Notably, MLMA cells showed the expression of CD10. When the expression of three types of receptors for BAFF was similarly examined, MLMA cells exhibited apparent expression of BAFF-R, while the levels of BCMA and TACI were found to be quite low (Fig. 1b). The data indicate that MLMA cells exhibit immunophenotypic characteristics of mature B cells expressing BAFF-R.

Cross-linking of BCR and CD20 induces apoptosis in MLMA cells

It has been well documented that cross-linking of BCR using anti-μ heavy chain antibodies induces apoptosis in some B cells *in vitro*.[25] Recent studies including our own have also shown that CD20 cross-linking mediates apoptosis in human B-cell lines in a manner involving raft-mediated signalling.[26,30] Therefore, we next examined whether cross-linking of either BCR or CD20 mediated apoptosis in MLMA cells. As shown in Fig. 2(a), when anti-μ antibodies were added to the culture, a time-dependent increase in the number of cells bound to annexin V was observed, suggesting the occurrence of apoptosis in MLMA cells after BCR cross-linking. The apoptosis was confirmed by the morphological appearance of nuclear fragmentation, a typical feature of apoptosis, detected by either Giemsa-staining or nuclear-staining with DAPI (Fig. 2b). Immunoblotting revealed the cleavage of caspases -9, -3 and -2 and of PARP after treatment with anti-μ antibodies (Fig. 2c), indicating that caspase activation was involved in the apoptosis. In the case of caspase-3, we also detected a 17 000 molecular weight cleaved fragment by using a specific antibody (Fig. 2c). In addition, elevation of the enzymatic activity of each caspase after cross-linking of BCR was detected by a colorimetric protease assay (Fig. 2d). We also examined the effect of anti-CD20 antibodies and found that CD20 cross-linking signalling induced apoptosis in MLMA cells (Fig. 2).

BAFF inhibits CD20-mediated and BCR-mediated apoptosis in MLMA cells

Next, we examined whether BAFF was able to inhibit apoptosis mediated by cross-linking of CD20 and BCR. As shown in Fig. 3(a), when BAFF was added to the

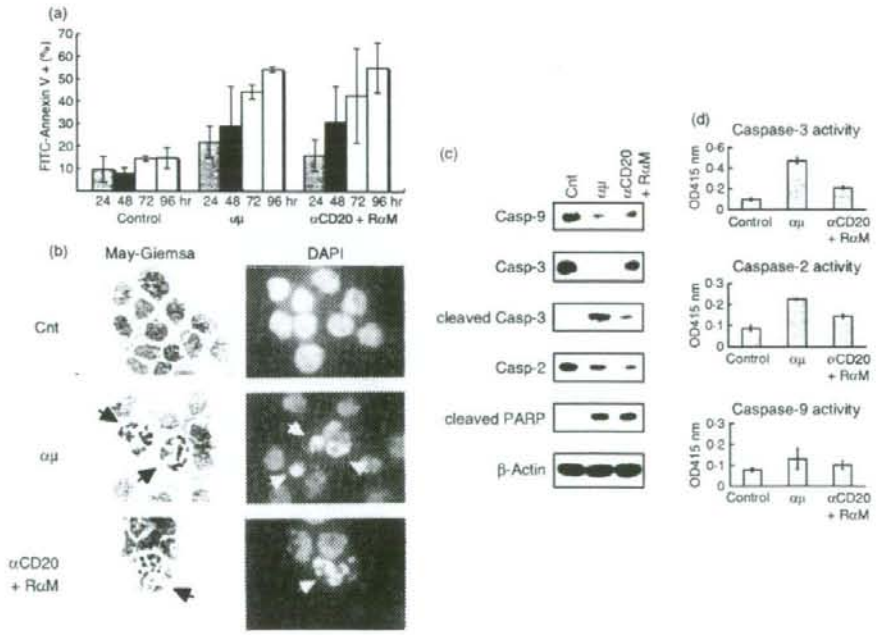

Figure 2. Induction of apoptosis in MLMA cells mediated by CD20 and B cell antigen receptor. (a) MLMA cells were treated with either rabbit anti-μ heavy-chain polyclonal antibody (αμ, 10 μg/ml) or a combination of anti-CD20 monoclonal antibody (mAb; αCD20, 5 μg/ml) and secondary rabbit anti-mouse immunoglobulin antibody (RαM, 5 μg/ml) for 48 hr and binding with fluorescein isothiocyanate (FITC)-conjugated annexin V was examined by flow cytometry. Each experiment was performed in triplicate and the means + SD are indicated. (b) The same sample preparations as in (a) were cytocentrifuged and morphological appearance was examined by Giemsa-staining and nuclear staining with DAPI, using light microscopy and confocal microscopy, respectively. (c) Cell lysates were obtained from the same sample preparation as in (a) and the proforms of each caspase, cleaved caspase 3 and cleaved PARP were detected by immunoblotting.

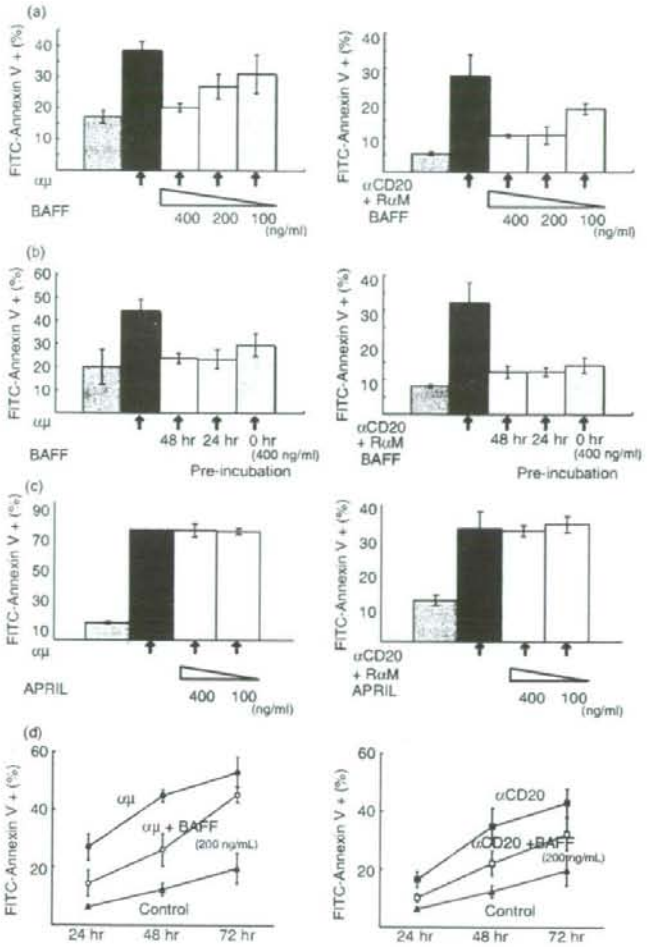

Figure 3. Effect of B cell activating factor (BAFF) on B cell receptor (BCR) induced and CD20 induced apoptosis in MLMA cells. (a) MLMA cells were treated with either rabbit anti μ heavy chain polyclonal antibody (mAb) (αμ, 10 μg/ml, left panel) or a combination of anti CD20 mAb (αCD20, 5 μg/ml) and secondary rabbit anti mouse immunoglobulin antibody (RαM, 5 μg/ml) (right panel) for 48 hr in the presence or absence of different concentrations of BAFF as indicated and binding with fluorescein isothiocyanate (FITC)-conjugated annexin V was examined as in Fig. 2(a). (b) MLMA cells preincubated with or without 400 ng/ml of BAFF for the indicated periods were treated with either αμ (left panel) or a combination of αCD20 and RαM (right panel) and examined as in (a). (c) The effect of APRIL on apoptosis induction was also examined as in (a). (d) MLMA cells were treated as in (a) and apoptosis was induced. The inhibitory effect of simultaneous addition of BAFF (200 ng/ml) against apoptosis was examined at different time points as in (a).

culture, the incidence of apoptosis induced by both BCR-mediated and CD20-mediated stimuli was reduced as assessed by annexin V-binding. Although inhibition tended to be more effective with a higher dose of BAFF, the effect was not significant. We also examined the effect of pretreatment with BAFF on the inhibition of apoptosis but found none (Fig. 3b). In contrast, APRIL, another ligand for BCMA and TACI, did not affect apoptosis induced by the BCR-mediated and CD20-mediated stimuli, indicating the specificity of BAFF's effect (Fig. 3c). Therefore, we concluded that BAFF-mediated stimuli are able to inhibit apoptosis mediated by the cross-linking of either CD20 or BCR and simultaneous treatment with apoptosis-inducing stimuli is almost sufficient to achieve maximum BAFF-mediated inhibition of apoptosis, at least in these cases. However, the inhibitory effect of BAFF against apoptosis mediated by the cross-linking of either CD20 or BCR was only partial and it was more obvious when the inhibition of apoptosis was examined at several different time-points.

Cellular effect of BAFF involved in the inhibition of apoptosis in MLMA cells

We further examined the molecular basis of the BAFF-mediated inhibition of apoptosis in MLMA cells. First, we tested the effect of BAFF on the growth of MLMA cells. As shown in Fig. 4, when BAFF was added to the culture, the cell proliferation was slightly enhanced, as assessed by cell counting, suggesting that BAFF promotes the growth of MLMA cells.

Next, we examined the intracellular signalling induced in MLMA cells by BAFF treatment. As shown in Fig. 5(a), immunoblot analysis revealed cleavage of p100, the precursor of NF-κB2, and a increase in p52, the active form of NF-κB2 after BAFF treatment, suggesting that the

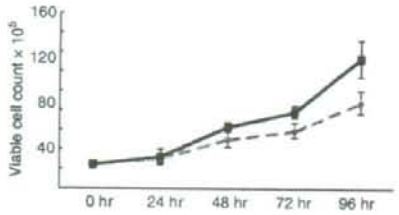

Figure 4. Effect of B-cell-activating factor (BAFF) on MLMA cell proliferation. Starting from a cell concentration at 5×10^5/ml, MLMA cells were cultured in the presence (solid line) and absence (dotted line) of 400 ng/ml of BAFF and cell numbers were counted at the time-points indicated. Each experiment was performed in triplicate and the means + SD are indicated.

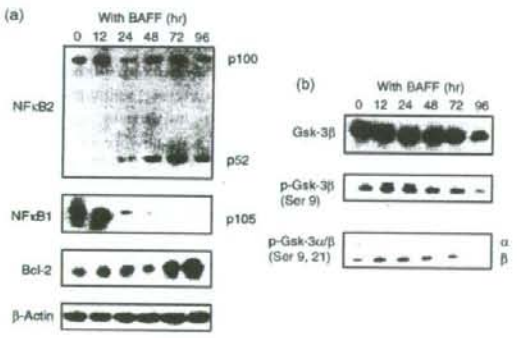

Figure 5. Intracellular signalling events and induction of Bcl-2 protein by B-cell activating factor (BAFF). Cell lysates were prepared from MLMA cells treated with 400 ng/ml of BAFF for the periods indicated and an immunoblot analysis was performed using the antibodies indicated.

activation of NF-κB2 occurred after the treatment. We also observed the cleavage of the precursor of NF-κB1 after BAFF treatment (Fig. 5a). We further examined the activation of other molecules after treatment with BAFF and found that GSK-3β was transiently phosphorylated (Fig. 5b). In addition, we observed an elevation in the level of Bcl-2, an anti-apoptotic protein, after BAFF treatment.

To investigate the early responses to BAFF in MLMA cells, global screening of candidate genes whose expression is regulated by BAFF was performed by employing a microarray system. First, we selected up-regulated genes that are expressed in MLMA cells treated with BAFF for 12 hr at a level at least 1·5-fold higher than in untreated cells. Under these conditions, 178 probes were selected as up-regulated genes (Table 1). Consistent with the results of the immunoblot analysis presented in Fig. 5(a), the gene expression of Bcl-2 was found to be up-regulated by BAFF treatment (Table 1). Interestingly, the gene expression of CD40, a member of the TNF-receptor family involved in B-cell survival, was also increased after treatment with BAFF. The genes that are known to be involved in anti-apoptotic effect, including *Myb*, Epstein–Barr virus (EBV)-induced gene 3 (*EBI3*), and caspase 8 and FADD-like apoptosis regulator (*CFLAR*), were also up-regulated by BAFF treatment.

We further confirmed the increased CD40 protein expression by flow cytometry (Fig. 6a). Similarly, down-regulated genes that were expressed in BAFF-treated cells at a level at least 0·75-fold lower than in untreated cells were selected. As shown in Table 2, 517 probes were selected as down-regulated genes. The above results of global gene expression profiling suggest that the expression of various types of genes was influenced by BAFF stimulation in MLMA cells.

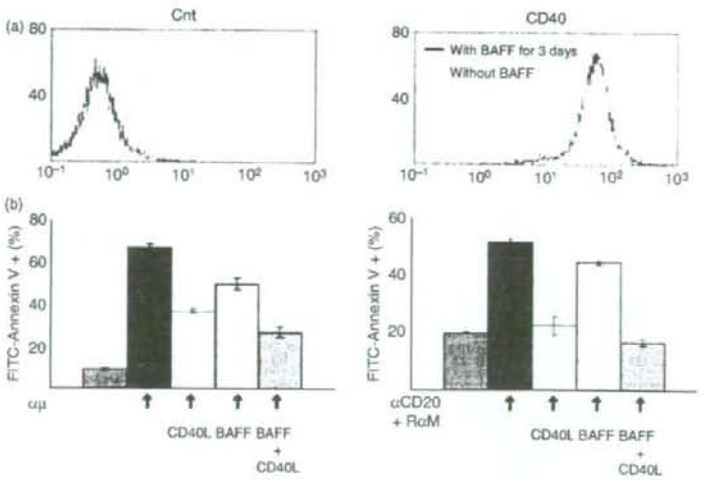

Figure 6. Effect of B-cell-activating factor (BAFF) on CD40 expression in MLMA cells. (a) MLMA cells cultured with or without BAFF for 3 days were stained with fluorescein isothiocyanate (FITC)-labelled monoclonal antibody (mAb) against CD40 and analysed by flow cytometry as in Fig. 1. (b) The inhibitory effect of CD40 stimulation on apoptosis induction was examined. MLMA cells were treated with 500 ng/ml of CD40-ligand in the presence of 2·5 ng/ml of interleukin-4 to stimulate CD40. The effects of either stimulation of CD40 alone or simultaneous stimulation of CD40 and BAFF receptor on apoptosis similarly induced as in Fig. 2 were examined.

Table 1. Up-regulated genes after BAFF stimulation

Affy ID	Gene name	Symbol	Fold-change
204798_at	V-myb myeloblastosis viral oncogene homolog	MYB	3·6934717
207861_at	Chemokine (C-C motif) ligand 22	CCL22	3·2195807
201669_s_at	Myristoylated alanine rich protein kinase C substrate	MARCKS	3·0888734
213138_at	AT rich interactive domain 5A	ARID5A	2·9730885
203927_at	IkBe	NFKBIE	2·6144874
239412_at	Interferon regulatory factor 5	IRF5	2·6300144
205173_x_at	CD58 antigen	CD58	2·5103657
230543_at	Similar to Chloride intracellular channel protein 4	USP9X	2·4929807
201932_at	Leucine rich repeat containing 41	MUF1	2·3778253
203835_at	Leucine rich repeat containing 32	GARP	2·3439856
221912_s_at	Human DNA sequence from clone RP4-622L5	MGC1203	2·296463
205599_at	TNF receptor associated factor 1	TRAF1	2·283286
218470_at	Tyrosyl-tRNA synthetase 2	CGI-04	2·2782216
203685_at	B-cell CLL/lymphoma 2	BCL2	2·2648098
202644_s_at	Tumor necrosis factor, alpha induced protein 3	TNFAIP3	2·2458956
204897_at	Prostaglandin E receptor 4 (subtype EP4)	PTGER4	2·2327275
217728_at	S100 calcium binding protein A6	S100A6	2·188896
234339_s_at	Glioma tumor suppressor candidate region gene 2	GLTSCR2	2·1786015
226354_at	Lactamase, beta	LACTB	2·1238286
209680_s_at	Kinesin family member C1	KIFC1	2·1163168
206508_at	Tumor necrosis factor (ligand) superfamily, member 7	TNFSF7	2·0985012
223319_at	Gephyrin	GPHN	2·0934505
242312_x_at	AV736963 CB		2·0774355
207608_x_at	Cytochrome P450, family 1, subfamily A, polypeptide 2	CYP1A2	2·019507
229437_at	BIC transcript	BIC	1·9920377
224468_s_at	Multidrug resistance related protein	MGC13170	1·9605879
214101_s_at	Aminopeptidase puromycin sensitive	NPEPPS	1·949555
208624_s_at	Eukaryotic translation initiation factor 4 gamma, 1	EIF4G1	1·9305304
218819_at	DEAD/H (Asp-Glu-Ala-Asp/His) box polypeptide 26	DDX26	1·925604
200648_s_at	Glutamate-ammonia ligase	GLUL	1·9081395
210686_x_at	Solute carrier family 25, member 16	GDA; GDC; ML7; hML7; HGT.1; D10S105E; MGC39851	1·903342
48659_at	Invasion inhibitory protein 45	FLJ12438	1·8990294
204283_at	Phenylalanine-tRNA synthetase 2	FARS2	1·8852582
1563796_s_at	KIAA1970 protein	KIAA1970	1·8749646
219424_at	Epstein-Barr virus induced gene 3	EBI3	1·8620349
213747_at	Antizyme inhibitor 1	OAZIN	1·8602847
205419_at	Epstein-Barr virus induced gene 2	EBI2	1·8580037
210978_s_at	Transgelin 2	TAGLN2	1·8418014
201502_s_at	IkBa	NFKBIA	1·8220907
207688_s_at	Inhibin, beta C	INHBC	1·8162365
208949_s_at	Lectin, galactoside-binding, soluble, 3	LGALS3	1·8159895
216252_x_at	Fas	FAS	1·7921783
203422_at	Polymerase (DNA directed), delta 1	POLD1	1·7856169
227299_at	Cyclin I	CCNI	1·7854006

Table 1. (*Continued*)

Affy ID	Gene name	Symbol	Fold change
218872_at	Hypothetical protein FLJ20607	TSC	1·7839508
205749_at	Cytochrome P450, family 1, subfamily A, polypeptide 1	CYP1A1	1·7801132
210514_x_at	HLA-G histocompatibility antigen, class I, G	HLA-G	1·780091
211376_s_at	Chromosome 10 open reading frame 86	C10orf86	1·7799767
212063_at	CD44 antigen	CD44	1·778577
201404_x_at	Proteasome (prosome, macropain) subunit, beta type, 2	PSMB2	1·774633
209939_x_at	CASP8 and FADD-like apoptosis regulator	CFLAR	1·7721851
225775_at	Tetraspanin 33	MGC50844	1·7708977
213642_at	Ribosomal protein L27	RPL27	1·7626065
209100_at	Interferon-related developmental regulator 2	IFRD2	1·7502396
201572_x_at	DCMP deaminase	DCTD	1·7400836
212642_s_at	Human DNA sequence from clone RP1-67K17	HIVEP2	1·7382044
221866_at		TFEB	1·7346125
204562_at	Interferon regulatory factor 4	IRF4	1·7332152
230660_at	SERTA domain containing 4	SERTAD4	1·7324636
229671_s_at	Chromosome 21 open reading frame 45	C21orf45	1·7187352
201797_s_at	Valyl tRNA synthetase	VARS2	1·7037842
212857_x_at	Similar to hypothetical protein DKFZp434P0316	PC4	1·7007011
225360_at	Hypothetical protein PP2447	PP2447	1·6819744
201565_s_at	Inhibitor of DNA binding 2	ID2	1·6807232
213113_s_at	Solute carrier family 43, member 3	SLC43A3	1·680492
212107_s_at	DEAH (Asp-Glu-Ala-His) box polypeptide 9	DHX9	1·6746678
204211_x_at	Eukaryotic translation initiation factor 2-alpha kinase 2	EIF2AK2	1·6744418
205153_s_at	CD40 antigen	CD40	1·6712306
214531_s_at	Sorting nexin 1	SNX1	1·6710757
226853_at	BMP2 inducible kinase	BMP2K	1·6657684
217734_s_at	WD repeat domain 6	WDR6	1·6582829
202418_at	Yip1 interacting factor homolog A	YIF1	1·6526384
203672_x_at	Thiopurine S-methyltransferase	TPMT	1·6522619
223287_s_at	Forkhead box P1	FOXP1	1·6494714
205621_at	AlkB, alkylation repair homolog	ALKBH	1·6476021
233310_at	Clone 25119 mRNA sequence		1·642435
201046_s_at	RAD23 homolog A	RAD23A	1·6409639
202161_at	Protein kinase N1	PKN1	1·6403072
219347_at	Nudix-type motif 15	NUDT15	1·6394255
226099_at	Elongation factor, RNA polymerase II, 2	ELL2	1·6393304
202715_at	Carbamoyl-phosphate synthetase 2,	CAD	1·6350683
214315_x_at	Calreticulin	CALR	1·6341119
227371_at	BAI1-associated protein 2-like 1	LOC55971	1·6332316
37028_at	Protein phosphatase 1, regulatory (inhibitor) subunit 15A	PPP1R15A	1·6298432
223079_s_at	Glutaminase	GLS	1·6280246
200613_at	Adaptor-related protein complex 2, mu 1 subunit	AP2M1	1·6246499
218611_at	Immediate early response 5	IER5	1·6235775
228993_s_at	Programmed cell death 4	PDCD4	1·6221018
224241_s_at	Homo sapiens cDNA clone IMAGE:2820510	PRO1855	1·6194851
205393_s_at	CHK1 checkpoint homolog	CHEK1	1·6177739
213826_s_at	H3 histone, family 3A	H3F3A	1·6139177
202819_s_at	Transcription elongation factor B (SIII), polypeptide 3	TCEB3	1·6136174
212064_x_at	MYC-associated zinc finger protein	MAZ	1·613094
218847_at	IGF-II mRNA-binding protein 2	IMP-2	1·6124035
201421_s_at	WD repeat domain 77	MEP50	1·6116982
230509_at	602041213F1 NCI_CGAP_Brn67	SNX22	1·610629
214383_x_at	Kelch domain containing 3	KLHDC3	1·604017
202265_at	Polycomb group ring finger 4	PCGF4	1·6002513

Table 1. (*Continued*)

Affy ID	Gene name	Symbol	Fold change
200894_s_at	FK506 binding protein 4, 59 kDa	FKBP4	1·5997517
202024_at	ArsA arsenite transporter, ATP binding, homolog 1	ASNA1	1·5976273
225625_at	Similar to hypothetical protein 9530023G02	MGC90512	1·5957043
224961_at	SCY1 like 2	SCYL2	1·5939683
222774_s_at	Neuropilin (NRP) and tolloid (TLL) like 2	NETO2	1·5898373
225063_at	Ubiquitin like 7 (bone marrow stromal cell-derived)	BMSC-UbP	1·5887783
218305_at	Importin 4	IPO4	1·5878817
204228_at	Peptidyl prolyl isomerase H (cyclophilin H)	PPIH	1·5876329
224966_s_at	Dihydrouridine synthase 3 like (S. cerevisiae)	LOC56931	1·5869961
239364_at	Ets variant gene 6 (TEL oncogene)	ETV6	1·5859513
206138_s_at	Phosphatidylinositol 4 kinase, catalytic, beta polypeptide	PIK4CB	1·5855292
209797_at	Transmembrane protein 4	TMEM4	1·5808252
204116_at	Interleukin 2 receptor, gamma	IL2RG	1·5777943
205965_at	Basic leucine zipper transcription factor, ATF-like	BATF	1·577366
201545_s_at	Poly(A) binding protein, nuclear 1	PABPN1	1·5768379
205235_s_at	M-phase phosphoprotein 1	MPHOSPH1	1·5718083
220924_s_at	Solute carrier family 38, member 2	SLC38A2	1·5694296
208858_s_at	Family with sequence similarity 62, member A	MBC2	1·5689234
203235_at	Thimet oligopeptidase 1	THOP1	1·5672989
215001_s_at	Glutamate ammonia ligase (glutamine synthetase)	GS; GLNS	1·5667295
224571_at	Interferon regulatory factor 2 binding protein 2	IRF2BP2	1·566219
235759_at	EF hand calcium binding protein 1	EFCBP1	1·5627139
218092_s_at	HIV-1 Rev binding protein	HRB	1·5555688
244413_at	Dendritic cell associated lectin 1	DCAL1	1·5547262
209781_s_at	KH domain containing, RNA binding, signal transduction associated 3	KHDRBS3	1·5527176
211965_at	Zinc finger protein 36, C3H type like 1	ZFP36L1	1·5514944
210740_s_at	Inositol 1,3,4-triphosphate 5/6 kinase	ITPK1	1·5482888
218097_s_at	CUE domain containing 2	CUEDC2	1·5461936
207618_s_at	BCS1-like	BCS1L	1·5440258
200628_s_at	Tryptophanyl tRNA synthetase	WARS	1·5433701
201490_s_at	Peptidylprolyl isomerase F (cyclophilin F)	PPIF	1·5432048
222425_s_at	Polymerase (DNA-directed), delta interacting protein 2	POLDIP2	1·5430135
240277_at	Solute carrier family 30 (zinc transporter), member 7	SLC30A7	1·5403106
204882_at	Rho GTPase activating protein 25	ARHGAP25	1·5393674
214784_x_at	Exportin 6	XPO6	1·5390915
201801_s_at	Solute carrier family 29 (nucleoside transporters), member 1	SLC29A1	1·5378566
202307_s_at	Transporter 1, ATP-binding cassette, sub-family B	TAP1	1·5369159
224913_s_at	Translocase of inner mitochondrial membrane 50 homolog	TIMM50	1·5356098
226797_at	Mbt domain containing 1	MBTD1	1·5314596
202887_s_at	DNA-damage-inducible transcript 4	DDIT4	1·53085
207396_s_at	Asparagine-linked glycosylation 3 homolog	ALG3	1·5305443
228487_s_at	Ras responsive element binding protein 1	RREB1	1·5286149
201473_at	Jun B proto-oncogene	JUNB	1·5285981
222968_at	Chromosome 6 open reading frame 48	C6orf48	1·5267475
203879_at	Phosphoinositide-3-kinase, catalytic, delta polypeptide	PIK3CD	1·5265557
206181_at	Signaling lymphocytic activation molecule family member 1	SLAMF1	1·5258498
238567_at	Sphingosine-1-phosphate phosphotase 2	SGPP2	1·5248299
223427_s_at	Erythrocyte membrane protein band 4·1 like 4B	EPB41L4B	1·5245888
215450_at	Small nuclear ribonucleoprotein polypeptide E	SNRPE	1·5239984
210428_s_at	Hepatocyte growth factor-regulated tyrosine kinase substrate	HGS	1·5230072
202968_s_at	Dual-specificity tyrosine-(Y)-phosphorylation regulated kinase 2	DYRK2	1·5226749
217289_s_at	glucose-6-phosphatase	G6PT; GSD1a	1·5194279
230466_s_at	Mesenchymal stem cell protein DSC96		1·5193534
229204_at	Heterochromatin protein 1, binding protein 3	HP1-BP74	1·5177599
223743_s_at	Mitochondrial ribosomal protein L4	MRPL4	1·5151922